PROPORTIONAL-INTEGRAL-DERIVATIVE (PID) CONTROLLER DESIGN FOR ROBUST STABILITY OF ARBITRARY ORDER PLANTS WITH TIME-DELAY AND ADDITIVE UNCERTAINTY

A Thesis By

Manoj Gogoi

Bachelor of Technology, B.P.U.T., India, 2007

Submitted to the Department of Electrical Engineering and Computer Science

and the faculty of the Graduate School of

Wichita State University

in partial fulfillment of

the requirements for the degree of

Master of Science

August 2010

©Copyright 2010 by Manoj Gogoi

All Rights Reserved

PROPORTIONAL-INTEGRAL-DERIVATIVE (PID) CONTROLLER DESIGN FOR ROBUST STABILITY OF ARBITRARY ORDER PLANTS WITH TIME-DELAY AND ADDITIVE UNCERTAINTY

The following faculty members have examined the final copy of this Thesis for form and content, and recommend that it be accepted in partial fulfillment of the requirement for the degree of Master of Science with a major in Electrical Engineering.

_____

John M. Watkins, Committee Chair

_____

Brain Driessen, Committee Member

_____

Tooran Emami, Committee Member

DEDICATION

To my parents, my younger sister, and my dear friends

ACKNOWLEDGEMENTS

I would like to take this opportunity to extend my gratitude towards my advisor and thesis committee chair Dr. John Watkins from the Electrical Engineering and Computer Science Department at Wichita State University for his continued support, guidance and motivation to complete this thesis. Working with Dr. Watkins was a joyful and educational experience.

I would like to extend my gratitude towards Dr. Tooran Emami from the Electrical and Computer Science Department for her continued encouragement, support, and motivation throughout my research. Dr. Emami guided me throughout this research and working with her was an excellent learning experience.

I take this opportunity to thank my supervisor Dr. Susan Matveyeva, who is an Associate Professor and Catalog and Institutional Repository Librarian for the Wichita State University Libraries, for believing in me and providing me financial support throughout my Master of Science program. I will also like to thank the entire Technical Service staff of the Wichita State University library.

I would also like to extend my gratitude towards Dr. Brain Driessen from the Mechanical Engineering Department, who served as one of my committee members. His reviews and comments were immensely helpful in the completion of my thesis.

ABSTRACT

In the process control industry, majority of control loops are based on Proportional-Integral-Derivative (PID) controllers. The basic structure of the PID controllers makes it easy to regulate the process output. Design methods leading to an optimal and effective operation of the PID controllers are economically vital for process industries. Robust control has been a recent addition to the field of control engineering that primarily deals with obtaining system robustness in presences of uncertainties. In this thesis, a graphical design method for obtaining the entire range of PID controller gains that robustly stabilize a system in the presence of time delays and additive uncertainty is introduced. This design method primarily depends on the frequency response of the system, which can serve to reduce the complexities involved in plant modeling. The fact that time-delays and parametric uncertainties are almost always present in real time processes makes our controller design method very vital for process control. We have applied our design method to a DC motor model with a communication delay and a single area non-reheat steam generation unit. The results were satisfactory and robust stability was achieved for the perturbed plants.

TABLE OF CONTENTS

Chapter Page

1. INTRODUCTION 1

1.1. Motivation.....1
1.2. Literature review.....2
1.3. Organization of the thesis……..……..3

2. BACKGROUND 4

2.1. Open-loop control systems 4
2.2. Closed-loop control systems 5
2.3. Multivariable control systems……..…….……..5
2.4. History of feedback control systems……...6
2.5. Proportional-Integral-Derivative (PID) control…….……..7
2.6. Robust control concepts……...…...8
2.7. Uncertainty and robust stability for SISO systems…….…...…10
2.7.1. Parametric uncertainty…….…….....11
2.7.2. Neglected and un-modeled dynamics ……..……..11
2.7.3. Lumped uncertainty…….……11
2.8. Time-delay systems……..13
2.9. Power generation control……....……14
2.9.1. Electrical machine basics…….……15
2.9.2. Power generation control systems……..……15
2.9.3. Primary governor control……..…...……17
2.9.4. Automatic generation control…….…..……..18

3. DESIGN METHODOLOGY…...…….……22

3.1. PID controller design in (K_p, K_i) plane for constant K_d ……..…...……..25
3.2. PID controller design in (K_p, K_d) plane for constant K_i ……...26
3.3. PID controller design in (K_i, K_d) plane for constant K_p ……...…28
3.4. PI controller design in (K_p, K_i) plane……..……..29

TABLE OF CONTENTS (continued)

Chapter Page

4. EXAMPLES……..……..……...31

4.1. PID controller design for a DC motor with time delay…….……31
4.1.1. Design goal…….…..31
4.1.2. Plant model……..….32
4.1.3. Designing additive uncertainty weight……...….32
4.1.4. Finding all PID controllers in (K_p, K_i) plane for constant K_d ……..….34
4.1.5. Finding all PID controllers in (K_p, K_d) plane for constant K_i ……...…37
4.1.6. Finding all PID controllers in (K_i, K_d) plane for constant K_p ……...……39
4.1.7. Conclusion……42
4.2. PI controller design for a single area non-reheat steam generator unit with additive uncertainty.....…43
4.2.1. Design goal.……...……...44
4.2.2. Plant model…….……..44
4.2.3. Additive uncertainty weight design…….…….47
4.2.4. PI controller design…….....51
4.2.5. Conclusion……52

5. CONCLUSION AND FUTURE WORK…….…….54

REFERENCES…….……...…….…….55

APPENDIXES…….……..59

APPENDIX A……60

MATLAB M-file for designing additive weight for DC motor with time delay

APPENDIX B……61

MATLAB M-file PID controller design to ensure robust stability in $(K_p, K_i), (K_p, K_d)$, and (K_i, K_d) plane for the DC motor model

TABLE OF CONTENTS (continued)

Chapter Page

APPENDIX C……69

MATLAB M-file for PID compensator design for DC motor (script file)

APPENDIX D……70

MATLAB M-file for PI controller design to ensure robust stability in (K_p, K_i) plane for the single area non-reheat steam generator unit

APPENDIX E……73

MATLAB M-file for designing additive weight (and script file) for the single area non-reheat steam generator unit

LIST OF TABLES

Table Page

1. Existing net summer capacity by energy source and producer type (USA), 2005 through 2008 (in megawatts)…….....14

2. Uncertain parameters……..48

3. Nominal plant parameters……..……..……...48

LIST OF FIGURES

Figure Page

1. Open loop control system……..……..……..4

2. Closed loop control system…….…...……5

3. Multivariable control system…….…….…..5

4. James Watt's fly ball governor……...……..…….6

5. PID control logic……...……...…….8

6. One degree-of-freedom feedback control system……...…….10

7. Plant with multiplicative uncertainty…….……...…11

8. Plant with additive uncertainty……..…..12

9. Time-delay system……..……..…13

10. Mechanical and electrical torques in a generating unit…….…….……..16

11. Primary and secondary control loops of a steam generator unit…….……...…17

12. Primary control with speed-droop feedback loop……...……..…18

13. Automatic generation control system with participating units…….……..19

14. LFC for a single area multiple generations……...…21

15. Block diagram of system with additive uncertainty weight……...…..22

16. DC motor model with time delay…….……31

17. Additive uncertainty representation for DC motor with time delay……..…...……..32

18. Additive weight representation……..……..……....34

19. Nominal stability boundary and robust stability region
for K_p and K_i values for $\overline{K_d} = 0.2$ …….……35

LIST OF FIGURES (continued)

Figure Page

20. Magnitude of $W_A(j\omega)K_i(j\omega)S(j\omega)$ for $K_1(s) = 3.6763 + \frac{3.0994}{s} + 0.2s$ and

$K_2(s) = 4.8675 + \frac{2.9825}{s} + 0.2s$ ……36

21. Nominal stability boundary and robust stability region
for K_p and K_d values for $\overline{K_i} = 1$ ……38

22. Magnitude of $W_A(j\omega)K_i(j\omega)S(j\omega)$ for $K_1(s) = 0.7869 + \frac{1}{s} - 0.2332s$ and

$K_2(s) = 1.6993 + \frac{1}{s} - 0.3130s$ ……39

23. Range of frequencies (ω_i) for $\overline{K_p} = 0.5$ ……40

24. Nominal stability boundary and robust stability region
for K_i and K_d values for $\overline{K_p} = 0.5$ ……41

25. Magnitude of $W_A(j\omega)K_i(j\omega)S(j\omega)$ for $K_1(s) = 0.5 + \frac{3.5311}{s} + 0.2456s$ and

$K_2(s) = 0.5 + \frac{4.5680}{s} + 0.2596s$ ……42

26. Block diagram representation of a single area non-reheat steam generation unit……45

27. Nominal model of a non-reheat steam generator unit……47

28. Additive uncertainty weight for single- area steam generator unit……50

LIST OF FIGURES (continued)

Figure Page

29. Nominal stability boundary and robust stability region in (K_p, K_i) plane……..……..….51

30. Magnitude of $W_A(j\omega)K(j\omega)S(j\omega)$ for $K(s) = 0.0338 + \frac{0.0040}{s}$ ……..….52

CHAPTER 1

INTRODUCTION

1.1 Motivation

Engineering is concerned with understanding and harnessing the forces of nature for the benefit of mankind while maintaining an ecological balance and a safe planet on which to live. Control engineering deals with understanding the plant under operation, and obtaining a desired output response in presence of system constraints. Due to the ample use of Proportional Integral Derivative (PID) controllers in process industry, there always has been a significant endeavor to obtain effective PID controller design methods, which will meet certain design criteria and provide system robustness. Controller design methods for Automatic Generation Control (AGC), a vital component of power system frequency control and generation scheduling, is being widely studied [1, 2, 15-20]. I am inspired by the fact that modern control engineering deals with improving manufacturing processes, efficiency of energy use, advanced automobile control, chemical processes, traffic control systems, and robotic systems, among others [3]. Integrating the basics of classical control, and the flexibilities offered by robust control, a new era of stable, sustainable, and reliable control systems can be designed. Plant parametric uncertainties and time-delays always tends to haunt production output and prevent optimal use of available resources. Robust control is concerned with obtaining control systems that are indifferent to model/plant mismatch or model uncertainty [4]. Extensive research has been done in controller design methods to obtain stability for plants with time-delay and uncertainties [5-14].

In this research, a graphical design method to obtain PI/PID controller gains to achieve robust stability for arbitrary order plants with time-delay and parametric uncertainties is discussed. Additive uncertainty modeling is used in order to obtain the entire uncertainty set.

The H_∞ controller design methodology is used to determine if the uncertain plant remains stable for the entire uncertainty set. The frequency domain application of this design method reduces the complexities of plant modeling. This controller design method is then applied to a DC motor model with time-delay and a single area non-reheat steam generator unit with parametric uncertainties. In the DC motor example, PID controller gains are found that will guarantee robust and closed loop stability. PI controller gains are obtained for the single area non-reheat steam generator unit in order to satisfy a robust stability constraint and obtain closed-loop stability.

1.2 Literature review

Much of the early works done in this area concentrated on finding PID controllers that stabilize a nominal plant model. Bhattacharyya and colleagues used a mathematical generalization of the Hermite-Biehler theorem to find all stabilizing PID controllers for systems with time-delay [6, 7, 8]. In [9, 10] an innovative controller design method, which did not required complex mathematical derivation, was presented. The authors of [9, 10] extended their research by obtaining the entire region of PID controllers that met certain gain and phase margin requirements. In [11, 12, 13, 14], techniques for finding all achievable PID controllers that stabilized an arbitrary order system and satisfied weighted sensitivity, complementary sensitivity, robust stability and robust performance constraints were introduced.

AGC influences the optimization of generator output, tie-line power interchange, customer billing, reducing Area Control Error (ACE), and the stability of a power operation system [1, 2, 15-20]. In [17], the authors described a method to reduce the mean value magnitude of the ACE below some threshold. A summary of the characteristics of a power generation system with AGC is presented in [15, 16]. In [17], a PI controller was designed for AGC of a two-area reheat thermal system where a new ACE formulation is presented. A genetic algorithm

(GA) method was used in [18] to optimize PI controller gains for a single area power system with multi-source power generation. In [19], a hybrid neuro fuzzy controller was designed for AGC of two interconnected power systems. In [20], the authors designed an H_∞ robust controller for single-input multiple-output (SIMO) non-linear hydro-turbine generation model. The goal of their paper was to stabilize the system in presence of uncertainties in the turbine-governor-load model.

1.3 Organization of the thesis

The remainder of the thesis is organized as follows. In Chapter 2, a general overview of the structure and applications of feedback control systems is presented. In this chapter, the most basic but vital robust control concepts of nominal stability, robust stability, and uncertainty modeling are reviewed. Furthermore, a general introduction of AGC and Load Frequency Control (LFC) is presented. In Chapter 3, the mathematical formulation of our proposed controller design method is presented. Application examples of this controller design method are presented in Chapter 4. Chapter 5 summarizes the results obtained in this research and highlights future research that can be done in the area of controller design.

CHAPTER 2

BACKGROUND

Control system engineers are concerned with controlling a part of an environment known as a plant or system in order to produce desired products for society. A prior knowledge of the plant to be controlled is often critical in designing effective control systems. The application of different engineering principles like that of electrical, mechanical, and/or chemical in order to achieve the desired output makes control engineering a multi-faceted engineering domain [3].

Control systems can be categorized as open-loop control or closed-loop feedback control systems depending on the system architecture and control method applied. Feedback control systems can be further differentiated as single-input-single-output (SISO) or multiple-input-multiple-output (MIMO), often called multivariable control systems [3].

2.1 Open-loop control systems

An open-loop control system is designed to meet the desired goals by using a reference signal that drives the actuators that directly control the process output. Output feedback is not present in this type of system. Figure 1 shows the general structure of an open-loop control system. A few examples of open-loop control systems are bread toasters, ovens, washing machines and water sprinkler systems [3].

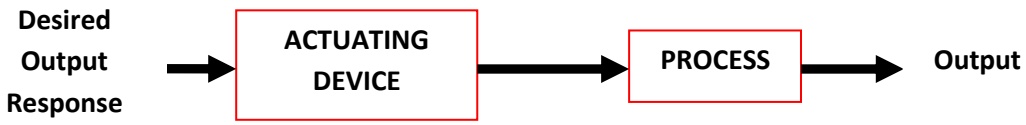

Figure 1. Open loop control system [3].

2.2 Closed-loop control systems

In closed-loop control systems the difference between the actual output and the desired output is fed back to the controller to meet desired system output. Often this difference, known as the error signal is amplified and fed into the controller. Figure 2 shows the general structure of a closed-loop feedback control system. A few examples of feedback control systems are elevators, thermostats, and the cruise control in automobiles [3].

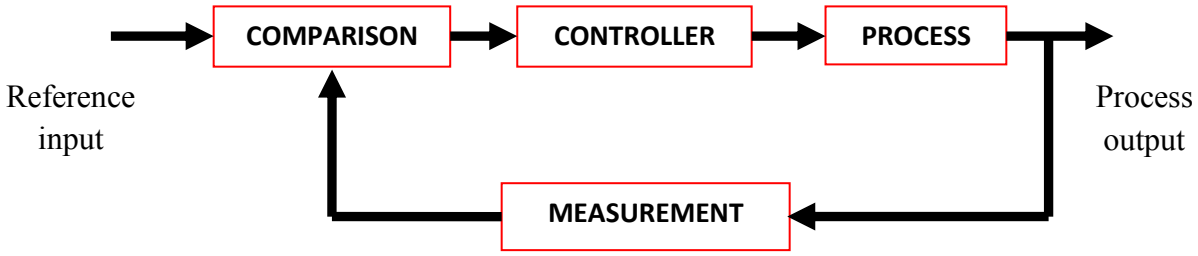

Figure 2. Closed loop control system [3].

2.3 Multivariable control systems

The increase in complexities of control systems involved and the interrelationship among process variables sometimes requires a multivariable feedback control system. A general structure of multivariable control system is shown in Figure 3.

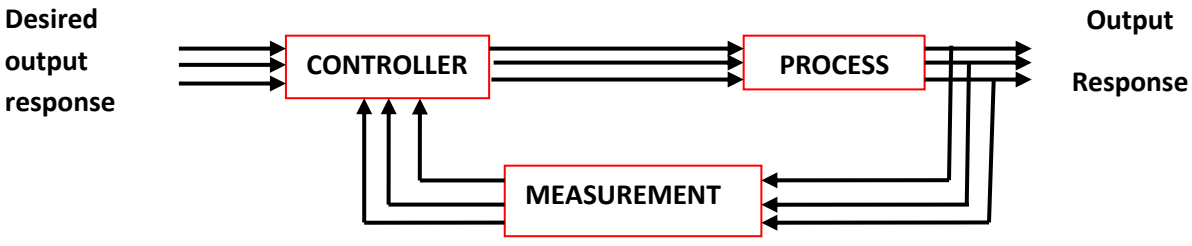

Figure 3. Multivariable control system [4].

2.4 History of feedback control systems

A feedback control system has had a fascinating history since its inception. The first known application of feedback control appeared when float regulator mechanisms were used in Greece in the period of 200 to 1 B.C. The first automatic feedback system was designed by Cornelis Drebbel [1572-1633] of Holland to regulate temperature. Dennis Papin [1647-1712] used feedback control theory to invent the first pressure regulator for steam boilers. The first feedback controller used in an industrial process, as accepted by most historians, was the invention of the fly ball governor, developed in 1769 by James Watt. This mechanism measured the speed of the output shaft and thereby utilized the movement of the fly ball in order to control the valve and thereby regulate the amount of steam entering the engine [3]. This feedback control mechanism is shown in Figure 4.

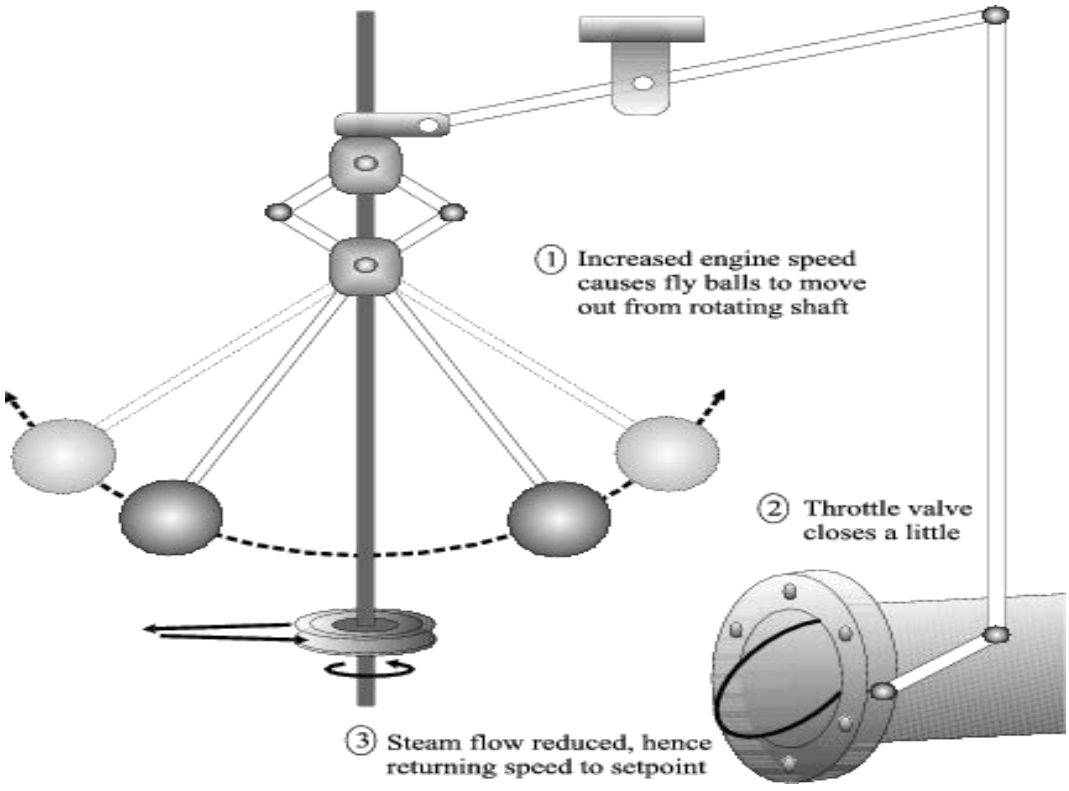

Figure 4. James Watt's fly ball governor [22].

Russian scientist I. Polzunov invented the water-level float regulator in 1765. During World War 2, there was a great focus on the development of military technologies that used the feedback control approach. In the 1950's s-plane methods like root locus were developed [3].

The space age, particularly with the Russian launch of Sputnik, lead to a new demand for complicated, highly accurate, and maneuverable control systems for missiles and space probes. This lead to the important field of optimal control, and increased interest in the time-domain methods. The 1980's saw the immergence of the very interesting and crucial robust control system approach [3].

2.5 Proportional-Integral-Derivative (PID) control

PID control logic is widely used in the process control industry. PID controllers have traditionally been chosen by control system engineers due to their flexibility and reliability [3].

A PID controller has proportional, integral and derivative terms that can be represented in transfer function form as

$$K(s) = K_p + \frac{K_i}{s} + K_d s \tag{1}$$

where K_p represents the proportional gain, K_i represents the integral gain, and K_d represents the derivative gain, respectively. By tuning these PID controller gains, the controller can provide control action designed for specific process requirements [3].

The proportional term drives a change to the output that is proportional to the current error. This proportional term is concerned with the current state of the process variable.

The integral term (K_i) is proportional to both the magnitude of the error and the duration of the error. It (when added to the proportional term) accelerates the movement of the process

towards the set point and often eliminates the residual steady-state error that may occur with a proportional only controller.

The rate of change of the process error is calculated by determining the differential slope of the error over time (i.e., its first derivative with respect to time). This rate of change in the error is multiplied by the derivative gain (K_d) [3].

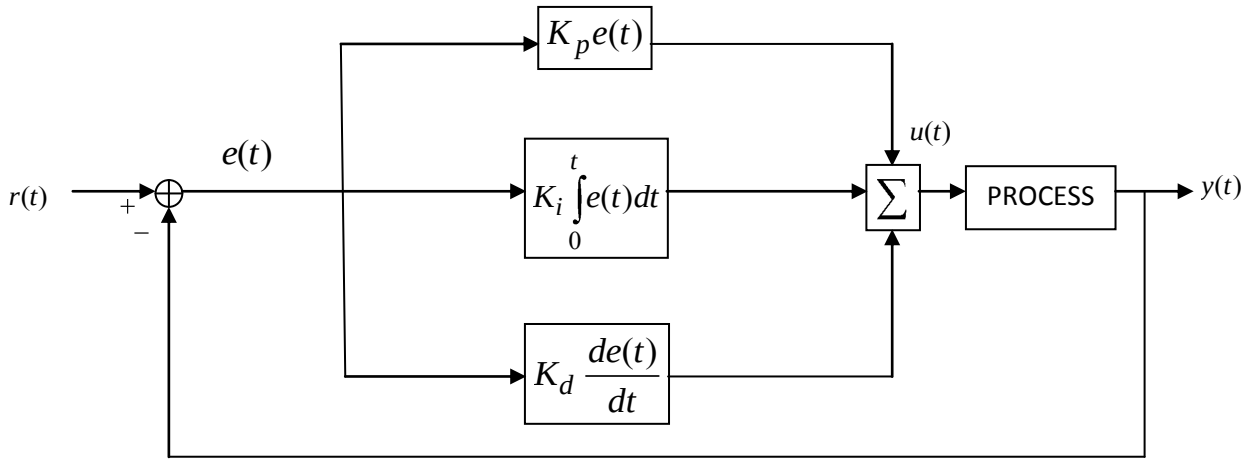

Figure 5. PID control logic.

2.6 Robust control concepts

Robust control is a branch of control theory that explicitly deals with uncertainty in its approach to controller design. Robust control methods aim at achieving robust stability and/or performance in the presence of uncertainties [4].

Loop shaping technique is an important classical controller design method [4]. During the 1980's the classical feedback control methods were extended to a more formal method based on shaping closed-loop transfer functions such as the weighted sensitivity function. These developments led to a more deep understanding of robust control concepts. Extensive research during this time paved the way for modern robust control concepts and its application to real-world systems [3].

Model uncertainty

A control system is robust if it is insensitive to differences between the actual system and the model of the system that was used to design the controller. These differences are referred to as model/plant mismatch or simply model uncertainty. Furthermore, as mentioned in [4], the key idea of H_∞ robust control is to check whether the design specifications are met for the "worst-case" uncertainty. The authors of [4] have taken the following approach to check robustness.

1. *Check nominal system stability.*
2. *Determine the uncertainty set*: Find a mathematical representation of the model uncertainty.
3. *Check Robust Stability (RS)*: Determine whether the system remains stable for all plants in the uncertainty set.
4. *Check Robust Performance (RP)*: If RS is satisfied; determine whether the performance specifications are met for all plants in the uncertainty set.

Figure 6 represents a general block diagram representation of a one degree-of-freedom feedback control system [4]. Here, *r* is the reference input, *u* is the control input to the plant, *y* is the actual plant output and *d* and *n* are the disturbance and noise signals respectively. *G*, G_d, and *K* are the plant model, disturbance model and controller respectively.

The objective of a control system is to make the output *y* behave in a desired way by manipulating *u* such that the control error e remains small in spite of the disturbance present. The system output can be denoted as [4],

$$y = G(s)u + G_d(s)d \tag{2}$$

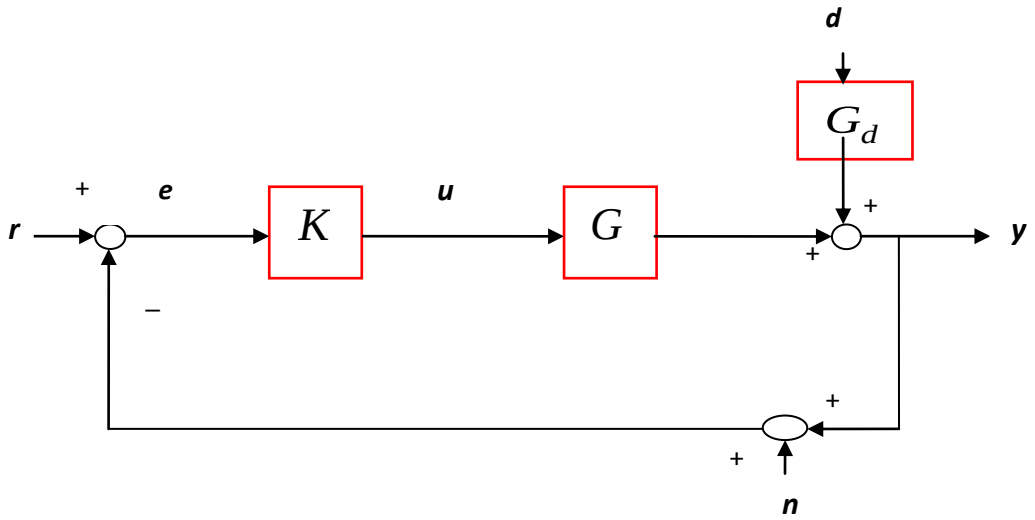

Figure 6. One degree-of-freedom feedback control system [4].

2.7 Uncertainty and robust stability for single-input-single-output (SISO) systems

As mentioned in Section 2.6, a robust control system always strives to remain insensitive towards the differences between the actual system and the model of the system that was used to design the control system. In this thesis, the primary goal is to find the set of PID controllers that will guarantee robust stability for any arbitrary order SISO plant in the presence of time-delay and/or additive uncertainties.

The origins of model uncertainty, as mentioned in [4], are as follows

1. Parameters in the linear model that are approximately known
2. Parameters that vary due to nonlinearities or changes in the operating conditions
3. Measurement devices often have imperfections
4. At high frequencies the structure and model order is often not known
5. Controller implemented may differ from the one obtained by solving the synthesis problem

Based on the above criteria, the main classes of model uncertainties are as follows

2.7.1 Parametric uncertainty

In this type of uncertainty the structure of the model is known, but some of the parameters are uncertain [4]. Here each uncertain parameter is bounded within some region $\delta_{\min}, \delta_{\max}$. This can be represented as,

$$\delta_p = \bar{\delta}(1 + r_p \Delta) \tag{3}$$

where $\bar{\delta}$ is the mean parameter value, $r_p = \dfrac{\delta_{\max} - \delta_{\min}}{\delta_{\max} + \delta_{\min}}$ is the relative uncertainty and Δ is a real scalar such that $|\Delta| \leq 1$ [4].

2.7.2 Neglected and un-modeled dynamics

In this class of uncertainty the model is in error because of missing dynamics, usually at high frequencies, either through neglect or lack of understanding of the process. A normalization technique which results in $\|\Delta\|_\infty \leq 1$ in the frequency domain, is typically applied [4].

2.7.3 Lumped uncertainty

Figure 7 shows a model of *multiplicative uncertainty* [4].

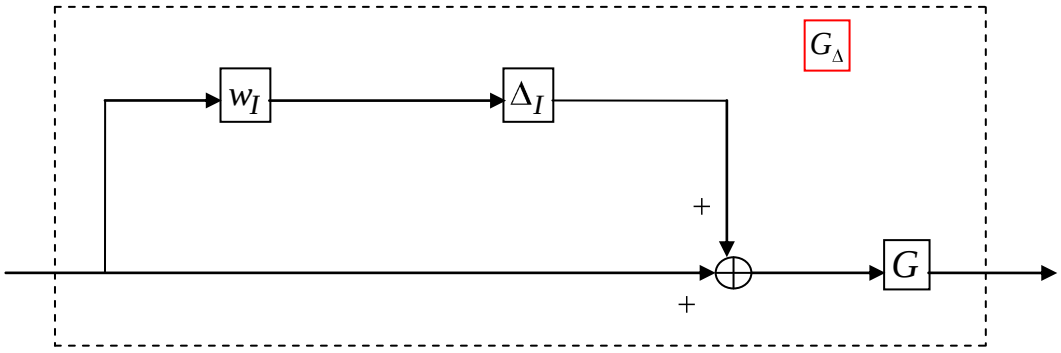

Figure 7. Plant with multiplicative uncertainty [4].

As mentioned in [4], this uncertainty description has one or more sources of parametric and/or unmodelled dynamics uncertainty that are combined into a single lumped perturbation of a chosen structure. Plants with *multiplicative uncertainty* can be mathematically represented as,

$$\pi_I : G_\Delta(j\omega) = G(j\omega)(1 + w_I(j\omega)\Delta_I(j\omega)) \;;\; \left|\Delta_I(j\omega)\right| \le 1 \forall \omega \tag{4}$$

where $G_\Delta(j\omega)$ represents the perturbed plant, $G(j\omega)$ is the nominal plant without uncertainty, $w_I(j\omega)$ is the multiplicative weight to be selected, and $\Delta_I(j\omega)$ is any stable transfer function such that $\forall\omega,\ \left|\Delta_I(j\omega)\right| \le 1$ [4].

In this thesis, an *additive uncertainty* modeling structure is chosen in order to bound the entire range of uncertainties. Figure 8 shows a model with *additive uncertainty.* In this figure, $G_\Delta(j\omega)$ represents the perturbed plant that bounds all the uncertainties, $G(j\omega)$ is the nominal plant without uncertainty, $w_A(j\omega)$ is the additive uncertainty weight, and $\Delta_A(j\omega)$ is any stable transfer function such that $\forall\omega,\ \left|\Delta_A(j\omega)\right| \le 1$ [4].

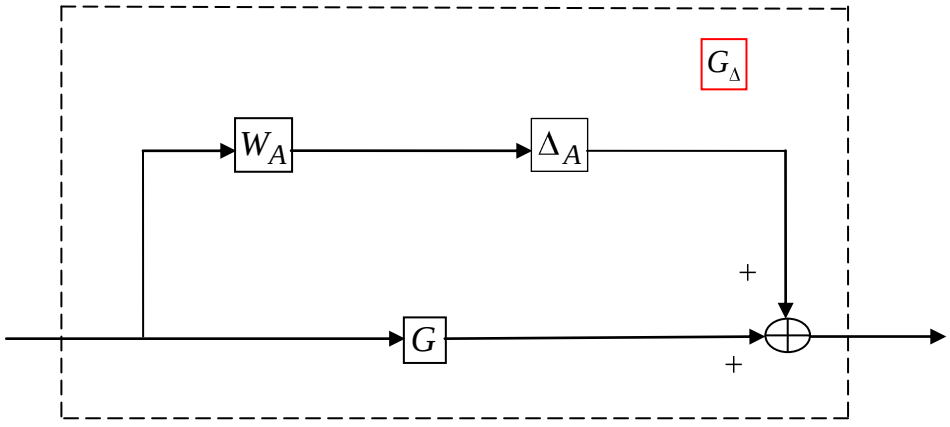

Figure 8. Plant with additive uncertainty [4].

Mathematically, plants with additive uncertainty are represented as,

$$\pi_A : G_\Delta(j\omega) = G(j\omega) + w_A(j\omega)\Delta_A(j\omega); \qquad |\Delta_A(j\omega)| \le 1 \forall \omega \qquad (5)$$

NOTE: A parametric representation of model uncertainty is sometimes called *structured uncertainty* as it includes uncertainty in a structured manner, while lumped uncertainty is often known as *unstructured uncertainty* [4].

2.8 Time-delay systems

It is to be noted that most real-time systems have time-delay associated with them. Time delay can originate due to one or more of the following reasons [21]:

1. Measurement of system variables
2. Physical properties of the equipment used in the system
3. Signal transmission (transport delay)

The effect of time delay on a system depends on the size of the delay and system characteristics. Systems where time delay plays a central role are control, economic, political, biological, and environmental systems. A few examples include a cold rolling mill, engine speed control, spaceship control, and hydraulic systems [21]. A block diagram representation of a cascade time delay system is shown in Figure 9.

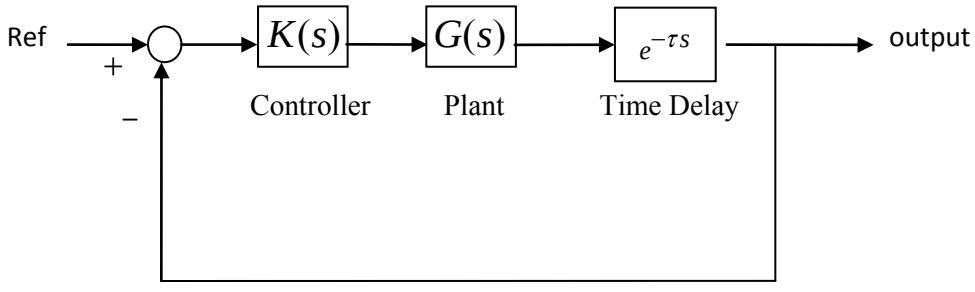

Figure 9. Time delay system

2.9 Power generation control

Electric energy represents an indispensable part of modern society. The law of energy conservation states that energy can neither be created nor destroyed; it can only be transformed from one state to another. Electricity is used in almost all spheres of modern life. Transportation, heating, lighting, communications, production and computation are just a few examples.

As stated by the independent statistics report of the *U.S. Energy Information Administration*, the total energy production capacity of United States as of 2008 was 1,010,171 megawatts (MW). The majority of this energy was generated from coal and natural gas. Table 1 shows a portion of the survey conducted by the agency [23].

TABLE 1

EXISTING NET SUMMER CAPACITY BY ENERGY SOURCE AND PRODUCER TYPE (USA), 2005 THROUGH 2008 (IN MEGAWATTS) [24]

	Coal	Petroleum	Natural Gas	Other Gases	Nuclear	Hydroelectric Conventional	Other Renewable	Hydroelectric Pumped Storage	Others	Total
2005	313,380	58,548	383,061	2,063	99,988	77,541	21,205	21,347	887	978,020
2006	312,956	58,097	388,294	2,256	100,334	77,821	24,113	21,461	882	986,215
2007	312,738	56,068	392,876	2,313	100,266	77,885	30,069	21,886	788	994,888
2008	313,322	57,445	397,432	1,995	100,755	77,930	38,493	21,858	942	1,010,171

Non-renewable energy sources such as coal, natural gas, and nuclear fuel are burned in a combustor to produce heat, which is in turn converted into mechanical energy in a turbine (also

known as prime mover). Alternative energy sources like wind and water are transformed into mechanical energy that is further converted to electrical energy with the help of electric machines [1]. The cost involved in the entire generation, safety, and transmission process demands a robust control system for effective power system operation.

2.9.1 Electrical machine basics

1. Electric machines are a set of magnetically and electrically coupled electric circuits that convert electric energy into mechanical energy or vice versa (generator mode).
2. An electrical machine can also be used to convert between different AC voltage levels [24].
3. From Faraday's law of electromagnetic induction we understand that the induced electromotive force (EMF) in any closed circuit is equal to the time rate of change of the magnetic flux through the circuit. This is given as,

$$\boxed{\left|emf\right| = N\left|\frac{d\phi_B}{dt}\right|} \tag{6}$$

where N is the number of turns of wire and $\emptyset_B$ is the magnetic flux in Weber's through a single loop. When the flux linkage $\left(\frac{d\phi_B}{dt} = 0\right)$ is constant, there is no electric energy transfer.

4. $\Delta P_m = T_e d\theta_r$ where ΔP_m is the mechanical energy change, T_e is the electro-magnetic torque, and $d\theta_r$ is the rotor angle increment [1].

2.9.2 Power generation control systems

A generator converts mechanical energy to electrical energy with the help of electromagnetic induction. It can be represented as a large rotating mass with two opposing torques. As shown in Figure 10, T_{mech} is the mechanical torque generated by the turbine and T_{elect} is the electrical

torque. T_{mech} tends to increase the rotational speed while T_{elect}, the electrical torque, tends to slow it down [1]. When $T_{mech} = T_{elect}$, the rotational speed ω is constant and equilibrium is achieved. If the electrical load is increased then $T_{elect} > T_{mech}$, which will cause the entire rotating system to slow down. In order to prevent equipment damage and meet the load demand an urgent increase in T_{mech} is necessary. This is vital to maintain system equilibrium. Due to frequent changes in load demand, this process of maintaining equilibrium is repetitive. Furthermore, due to the presence of different generator units supplying power to the transmission system, allocation of load change to these units is also important [1]. To achieve this goal, control systems are installed with the generator units for generation scheduling and LFC.

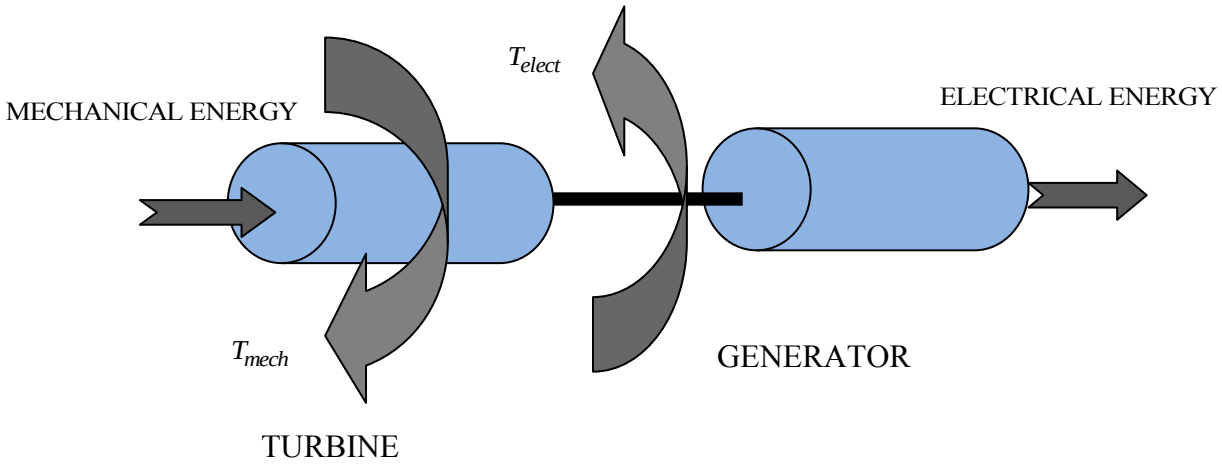

Figure 10. Mechanical and electrical torques in a generating unit [1].

Thus, a primary or governor control unit in each section tends to maintain the rotational speed, while a supplementary control scheme like AGC acts to distribute system generation among control areas in order to match the scheduled power interchange. This serves to match total system generation to total system load.

The primary control loop responds instantly to frequency deviations and brings the rate of change of frequency to zero within seconds [1]. The supplementary control scheme tends to regulate the LFC and the economic dispatch function. ACE is the input to the controller. In this thesis, a single area non-reheat steam turbine unit is studied [2]. Figure 11 shows the generation control scheme with both primary and secondary control loops.

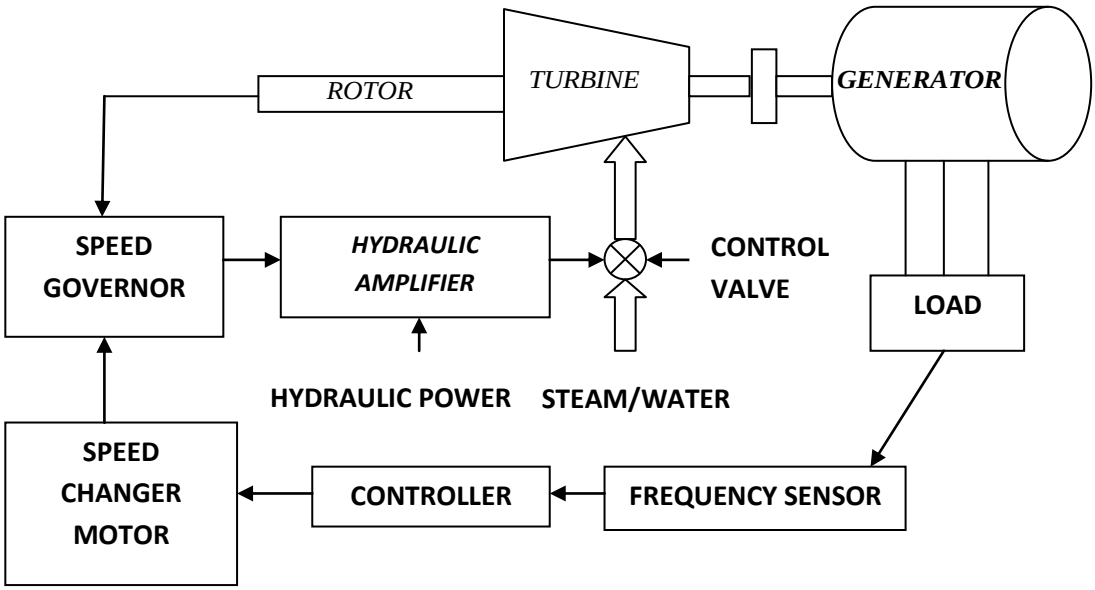

Figure 11. Primary and secondary control loops of a steam generator unit [2].

2.9.3 Primary governor control

In order to compensate a frequency sensitive load change with a change in mechanical power input a simple governing mechanism is added to each generator unit. This unit senses the machine speed and adjusts the input valve to change the mechanical power output. This compensates the load change that has occurred and the frequency is adjusted back to its nominal value. This forms the primary response loop for speed change regulation of the electric machine [1].

As mentioned in [1], in order to achieve the nominal frequency by the governor, the governing mechanism needs to perform a reset action that is accomplished by integrating the frequency error, which is the difference between the designed and actual rotating speed and thereby feeding it into the control valve mechanism. This in turn opens the inlet valve to compensate for the speed change with the increase in mechanical input. Figure 12 shows a speed governing mechanism with speed-droop feedback [1].

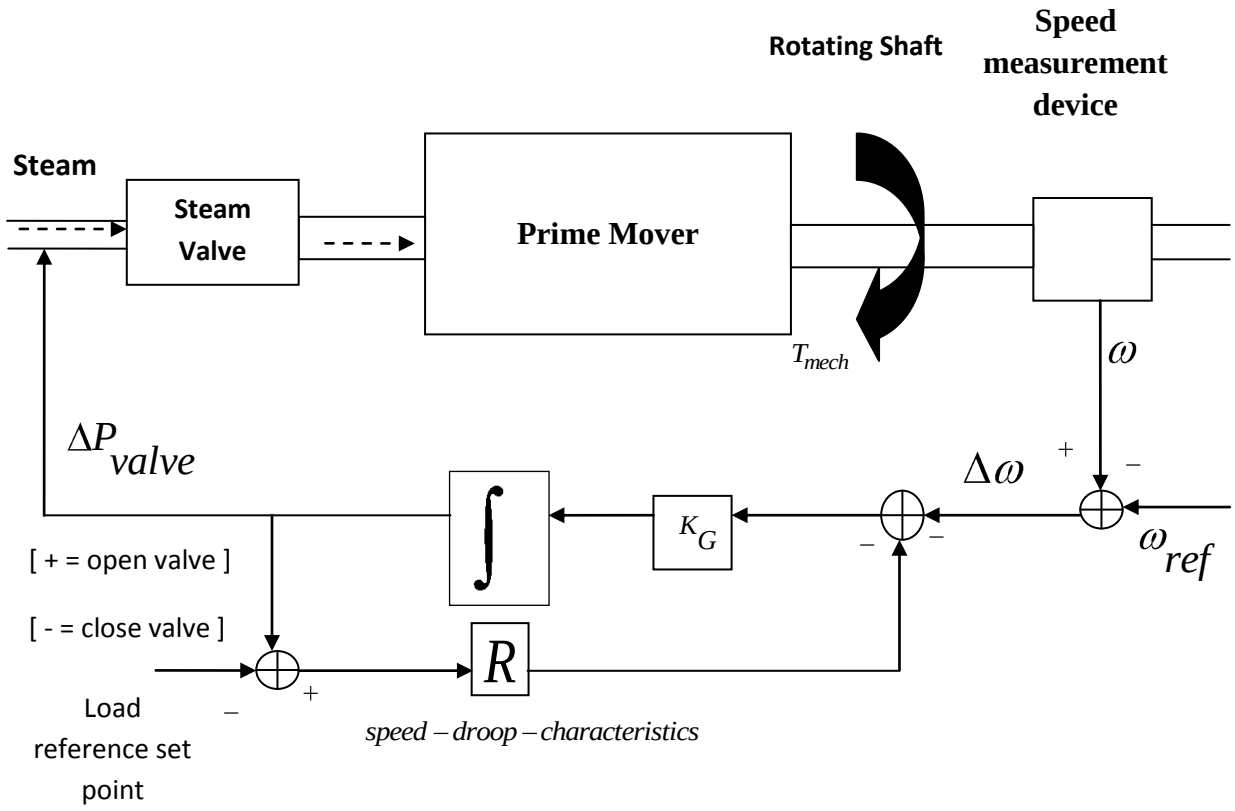

Figure 12. Primary control with speed-droop feedback loop [1]

2.9.4. Automatic generation control

If we assume that each control area in a interconnected power system had a single generating unit, as shown in Figure 11, then the control system would have been able to directly stabilize the system frequency with a change in load and maintain a tie-line interchange. But in real-world there exist numerous control areas with more generating units with outputs that must be set according to economic dispatch [2]. Furthermore, as there are frequent changes in load it is

un- realistic to specify the amount of unit output for each unit. This has led to the need of an AGC control scheme that will enable scheduled MW production and distribution among generation units. AGC schemes are managed at a central location where information is telemetered to the controlled areas. Control actions are generated in a digital computer before being transmitted to the generation units [2]. This AGC scheme is illustrated in Figure 13.

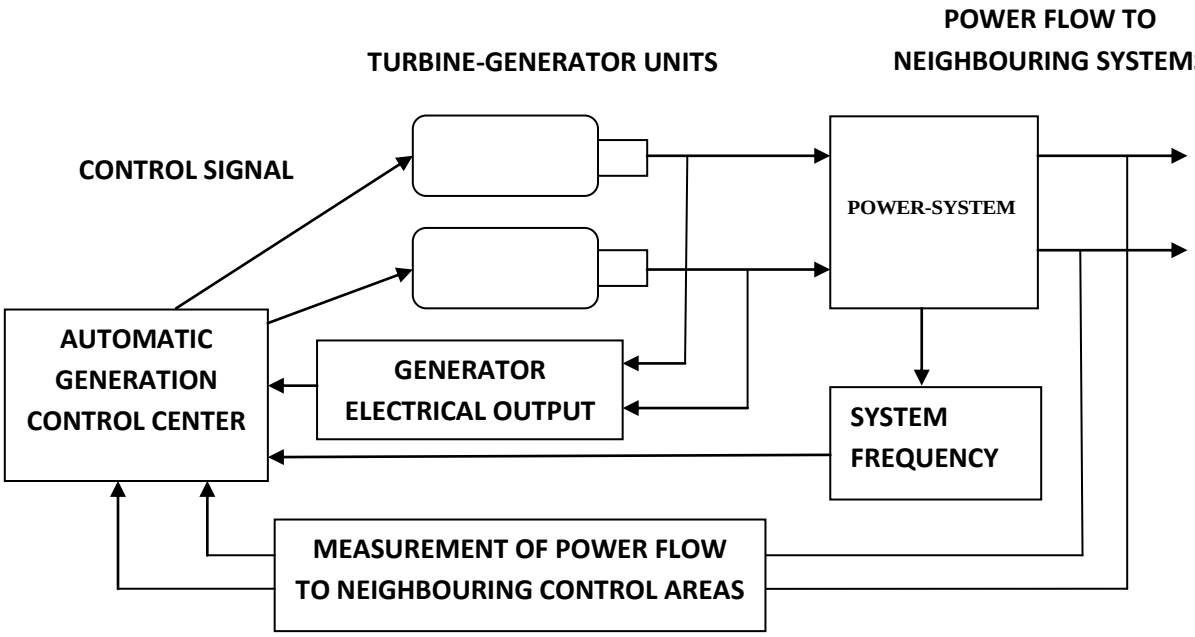

Figure 13. Automatic generation control system with participating units [1].

The primary goal of AGC is to match consumer load demand with the generator electrical output. As mentioned in [1, 2, 15, 16, 17], AGC is a control scheme that has three major objectives.

1. Maintain system frequency at or close to a specified nominal value (e.g. 60 Hz)
2. Maintain correct and scheduled value of power interchange between interconnected control areas
3. Maintain each unit's generation output at the most economical value

Thus, AGC effects the optimization of generator output, tie-line power interchange, customer billing, reducing ACE, and stability of a power operation system.

ACE_i represents the real power imbalance between generation and load for control area *i*. ACE_i represents a linear combination of net interchange and frequency deviations. This is represented as [1, 2],

$$ACE_i = \Delta P_{net} + B_i \Delta\omega \tag{7}$$

where ΔP_{net} is the net power interchange, $\Delta\omega$ is the frequency change, and B_i represents the frequency bias factor that is given by ,

$$B_i = \frac{1}{R_i} + D_i \tag{8}$$

ACE is the input to the controller (predominantly PI). The resulting output control signal is conditioned by limiters, delays and a gain constant, which is further distributed among participant generation unit in accordance with their participation factors [1, 2].

An AGC scheme for multiple interconnected generation areas is shown in Figure 14. The main goal of the control system is to maintain nominal system frequency and manage power interchange within scheduled value [2].

The entire process of LFC for a single-area with multiple generation units is shown in Figure 14. For control area *i*, $K_i(s)$ is the designed controller, α_{ki} is the participation factor for generation unit *k*, M_{ki} is the combine governor-turbine transfer function model for generator unit *k*, B_i is the frequency bias factor, and R_{ki} is the speed-droop characteristics for generation unit *k*. Furthermore, Δf_i is the frequency change for control area *i*, Δf_j is the frequency change in

interconnected control area j, ΔP_{c_i} is the control input, $\sum_{\substack{j=1 \\ j\neq 1}}^{N} T_{ij}$ is the total tie line interchange between control areas i and j, ΔP_L is the load change experienced by this area, and $2\pi/s$ is the integral gain added to the feedback loop.

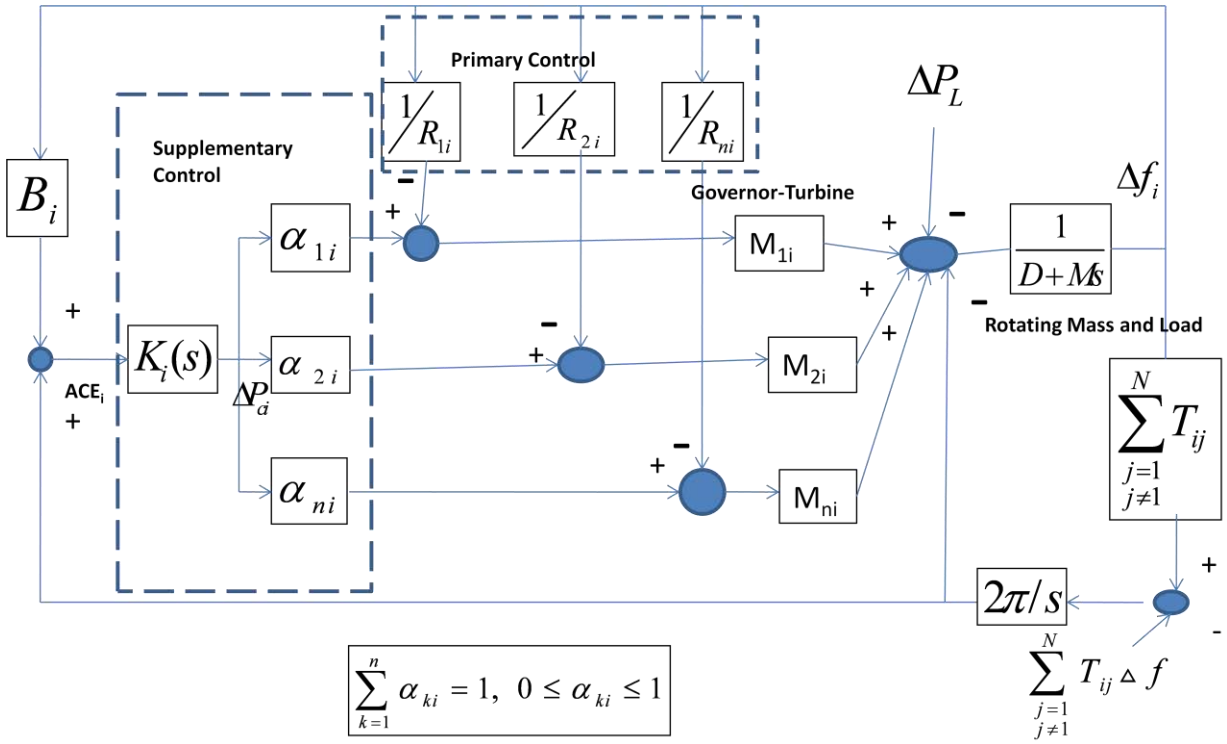

Figure 14. Load frequency control for a single-area multiple generations [2].

In this thesis, a PI controller design method for a single-area single generation non-reheat steam generator unit with parametric uncertainties will be presented. The nominal stability boundary and robust stability region for the PI controller gains will be obtained. It will be shown that the simulation results are satisfactory as the robust stability constraint is satisfied. The practical application of this controller design method is important for power-generation control.

CHAPTER 3

DESIGN METHODOLOGY

In this chapter, we will discuss the mathematical formulations that are most vital in order to obtain the set of PID controller gains that will enable us to obtain the nominal stability boundary and robust stability region for an arbitrary order perturbed plant with additive uncertainty, while ensuring closed loop stability.

In Figure 15, a SISO and linear time invariant (LTI) system with additive uncertainty is shown. Here $G_p(s)$ is the nominal plant, $K(s)$ is the PID controller, and $W_A(s)$ is the additive weight. The input signal and the weighted output signal are $R(s)$ and $Z(s)$ respectively [4].

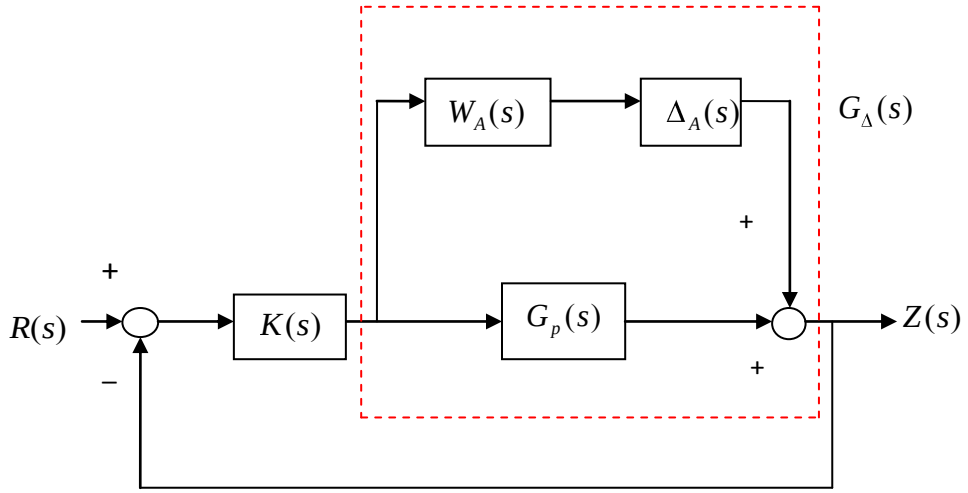

Figure 15. Block diagram of system with additive uncertainty weight [4].

In Figure 15, $G_\Delta(s)$ represents the perturbed plant which includes $\Delta_A(s)$, which is any stable transfer function such that $|\Delta_A(j\omega)| \le 1, \ \forall \omega$. In the frequency domain we can represent these transfer functions as

$$G_p(j\omega) = \mathrm{Re}(\omega) + j\,\mathrm{Im}(\omega) \tag{9}$$

$$K(j\omega) = K_p + \frac{K_i}{j\omega} + K_d\, j\omega \tag{10}$$

$$W_A(j\omega) = A_A(\omega) + jB_A(\omega) \tag{11}$$

In order to achieve robust stability for the perturbed system, we want to find all PID controller gains that stabilize the closed loop system for the entire range of uncertainties. This goal can be achieved if the nominal system is stable and the robust stability constraint

$$\left\| W_A(j\omega)K(j\omega)S(j\omega) \right\|_\infty \le \gamma \tag{12}$$

is satisfied, where $S(j\omega)$ is the sensitivity function and $\gamma = 1$

$$S(j\omega) = \frac{1}{1 + G_p(j\omega)K(j\omega)} \tag{13}$$

The weighted sensitivity constraint of the SISO system can be represented in its magnitude and phase as;

$$W_A(j\omega)K(j\omega)S(j\omega) = \left| W_A(j\omega)K(j\omega)S(j\omega) \right| e^{j\angle W_A(j\omega)K(j\omega)S(j\omega)} \tag{14}$$

The robust stability constraint can be rewritten as

$$W_A(j\omega)K(j\omega)S(j\omega)e^{j\theta_A} \le \gamma \;\forall\omega \tag{15}$$

or

$$\frac{W_A(j\omega)K(j\omega)}{1 + G_p(j\omega)K(j\omega)} e^{j\theta_A} \le \gamma \;\forall\omega \tag{16}$$

where $\theta_A = -\angle W_A(j\omega)K(j\omega)S(j\omega)$.

Thus equation (16) should be satisfied for some values of $\theta_A \in [0, 2\pi]$. All PID controllers that would satisfy equation (12) have to lie at the intersection of all controllers that satisfy equation (15) for all $\theta_A \in [0, 2\pi]$.

For each value of $\theta_A \in [0, 2\pi]$ we will find all PID controllers on the boundary of equation (16). It can shown from equation (16), that all the PID controllers on the boundary must satisfy

$$P(\omega, \theta_A, \gamma) = 0 \tag{17}$$

where the characteristic polynomial $P(\omega, \theta_A, \gamma)$ can be represented as

$$P(\omega, \theta_A, \gamma) = 1 + G_p(j\omega)K(j\omega) - \frac{1}{\gamma}\left\{ W_A(j\omega)K(j\omega)e^{j\theta_A} \right\} \tag{18}$$

Now, by substituting the frequency responses represented by equation (9), equation (10), equation (11), and $e^{j\theta_A} = \cos\theta_A + j\sin\theta_A$ into equation (18) we obtain

$$\begin{aligned} P(\omega, \theta_A, \gamma) = 1 + &\left((\mathrm{Re}\ \omega\ + j\,\mathrm{Im}(\omega)) \left(K_p + \frac{K_i}{j\omega} + K_d\, j\omega \right) \right) - \\ &\left(\frac{1}{\gamma}(A_A(\omega) + jB_A(\omega)) \left(K_p + \frac{K_i}{j\omega} + K_d\, j\omega \right) (\cos\theta_A + j\sin\theta_A) \right) \end{aligned} \tag{19}$$

For $\gamma \to \infty,$ equation (19) reduces to the general characteristic polynomial.

Thus, the nominal stability boundary can be obtained for $\gamma \to \infty$.

Expanding equation (17) into real and imaginary parts yields

$$\begin{aligned} X_{R_p} K_p + X_{R_i} K_i + X_{R_d} K_d &= 0 \\ X_{I_p} K_p + X_{I_i} K_i + X_{I_d} K_d &= -\omega \end{aligned} \tag{20}$$

where the real components are given by

$$
\begin{aligned}
X_{R_p} &= -\omega\left(\mathrm{Im}(\omega)+\frac{1}{\gamma}(A_A\sin\theta_A+B_A\cos\theta_A)\right)\\
X_{R_i} &= \left(\mathrm{Re}(\omega)+\frac{1}{\gamma}(A_A\cos\theta_A-B_A\sin\theta_A)\right)\\
X_{R_d} &= -\omega^2\left(\mathrm{Re}(\omega)+\frac{1}{\gamma}(A_A\cos\theta_A-B_A\sin\theta_A)\right)
\end{aligned}
\tag{21}
$$

and, the imaginary components are given by

$$
\begin{aligned}
X_{I_p} &= \omega\left(\mathrm{Re}(\omega)+\frac{1}{\gamma}(A_A\cos\theta_A-B_A\sin\theta_A)\right)\\
X_{I_i} &= \left(\mathrm{Im}(\omega)+\frac{1}{\gamma}(A_A\sin\theta_A+B_A\cos\theta_A)\right)\\
X_{I_d} &= -\omega^2\left(\mathrm{Im}(\omega)+\frac{1}{\gamma}(A_A\sin\theta_A+B_A\cos\theta_A)\right)
\end{aligned}
\tag{22}
$$

3.1 PID controller design in (K_p, K_i) plane for constant K_d

The boundary for $P(\omega,\theta_A,\gamma)=0$ for the (K_p,K_i) plane for a fixed value of $K_d=\overline{K_d}$ is found using equation (20), which can rewritten as

$$
\begin{bmatrix} X_{R_p} & X_{R_i} \\ X_{I_p} & X_{I_i} \end{bmatrix}\begin{bmatrix} K_p \\ K_i \end{bmatrix}=\begin{bmatrix} 0-X_{R_d}\,\overline{K_d} \\ -\omega-X_{I_d}\,\overline{K_d} \end{bmatrix} \tag{23}
$$

Solving equation (23) for all ω≠0 and $\theta_A\in[0,2\pi]$, we obtain the controller gains as

$$
K_p(\omega,\theta_A,\gamma)=\frac{-\mathrm{Re}(\omega)-\frac{1}{\gamma}(A_A\cos\theta_A-B_A\sin\theta_A)}{X(\omega)} \tag{24}
$$

$$K_I(\omega,\theta_A,\gamma)=\omega^2\overline{K_d}+\frac{-\omega\left(\mathrm{Im}(\omega)+\frac{1}{\gamma}(A_A\sin\theta_A+B_A\cos\theta_A)\right)}{X(\omega)} \tag{25}$$

where

$$X(\omega)=\left|G_p(j\omega)\right|^2+\frac{1}{\gamma^2}\left|W_A(j\omega)\right|^2+\frac{2}{\gamma}\begin{pmatrix}\mathrm{Re}(\omega)(A_A\cos\theta_A-B_A\sin\theta_A)\\+\mathrm{Im}(\omega)(A_A\sin\theta_A+B_A\cos\theta_A)\end{pmatrix}$$

$$\begin{aligned}\left|G_p(j\omega)\right|^2&=\mathrm{Re}^2(\omega)+\mathrm{Im}^2(\omega)\\\left|W_A(j\omega)\right|^2&=A_A{}^2(\omega)+B_A{}^2(\omega)\end{aligned} \tag{26}$$

Setting $\omega=0$ in equation (23), we obtain

$$\begin{bmatrix}0 & X_{R_i}(0)\\0 & X_{I_i}(0)\end{bmatrix}\begin{bmatrix}K_p\\K_i\end{bmatrix}=\begin{bmatrix}0\\0\end{bmatrix} \tag{27}$$

and conclude that $K_p(0,\theta_A,\gamma)$ is arbitrary and $K_i(0,\theta_A,\gamma)=0$ unless Im(0) = Re(0) = 0, which holds only when $G_p(s)$ has a zero at the origin.

3.2 PID controller design in (K_p,K_d) plane for constant K_i

The boundary for $P(\omega,\theta_A,\gamma)=0$ for the (K_p,K_d) plane for a fixed value of $K_i=\overline{K_i}$ is found using equation (20), which can be rewritten as

$$\begin{bmatrix}X_{R_p} & X_{R_d}\\X_{I_p} & X_{I_d}\end{bmatrix}\begin{bmatrix}K_p\\K_d\end{bmatrix}=\begin{bmatrix}0-X_{R_i}\overline{K_i}\\-\omega-X_{I_i}\overline{K_i}\end{bmatrix} \tag{28}$$

Solving equation (28) for all ω≠0 and $\theta_A \in 0, 2\pi$, we obtain the controller gains as,

$$K_p(\omega,\theta_A,\gamma) = \frac{-\mathrm{Re}(\omega) - \frac{1}{\gamma}(A_A \cos\theta_A - B_A \sin\theta_A)}{X(\omega)} \tag{29}$$

and

$$K_d(\omega,\theta_A,\gamma) = \frac{\overline{K_i}}{\omega^2} + \frac{\mathrm{Im}(\omega) + \frac{1}{\gamma}(A_A \sin\theta_A + B_A \cos\theta_A)}{\omega X(\omega)} \tag{30}$$

where,

$$X(\omega) = \left|G_p(j\omega)\right|^2 + \frac{1}{\gamma^2}\left|W_A(j\omega)\right|^2 + \frac{2}{\gamma}\begin{pmatrix} \mathrm{Re}(\omega)(A_A \cos\theta_A - B_A \sin\theta_A) \\ +\mathrm{Im}(\omega)(A_A \sin\theta_A + B_A \cos\theta_A) \end{pmatrix} \tag{31}$$

Equation (28) can be rewritten as

$$\begin{bmatrix} -\omega\alpha(\omega) & -\omega^2\beta(\omega) \\ \omega\beta(\omega) & -\omega^2\alpha(\omega) \end{bmatrix}\begin{bmatrix} K_p \\ K_d \end{bmatrix} = \begin{bmatrix} 0 - X_{R_i}\overline{K_i} \\ -\omega - X_{I_i}\overline{K_i} \end{bmatrix} \tag{32}$$

where,

$$\alpha(\omega) = \left(\mathrm{Im}(\omega) + \frac{1}{\gamma}(A_A(\omega)\sin\theta_A + B_A(\omega)\cos\theta_A)\right)$$

$$\beta(\omega) = \left(\mathrm{Re}\ \omega\ + \frac{1}{\gamma}(A_A(\omega)\cos\theta_A - B_A(\omega)\sin\theta_A)\right)$$

For $\omega = 0$ a solution may exist if $\overline{K_i} = 0.$ Solving

$$\begin{bmatrix} -\alpha(0) & 0 \\ \beta(0) & 0 \end{bmatrix}\begin{bmatrix} K_p \\ K_d \end{bmatrix} = \begin{bmatrix} 0 \\ -1 \end{bmatrix} \tag{33}$$

we obtain $-\alpha(0)K_p = 0$ and $\beta(0)K_p = -1.$

we conclude $K_d(0,\theta_A,\gamma)$ is arbitrary and

$$K_p(0,\theta_A,\gamma)=\frac{-1}{\overline{\beta(0)}}=\frac{-1}{\mathrm{Re}(0)+\frac{1}{\gamma}(A_A(0)\cos\theta_A-B_A(0)\sin\theta_A)} \tag{34}$$

if $\alpha(0)=0$ and $\beta(0)\neq 0$.

3.3 PID controller design in (K_i,K_d) plane for constant K_p

For $K_p=\overline{K_p}$ (constant), equation (20) can be written as the coefficient matrix,

$$\begin{bmatrix} X_{R_i} & X_{R_d} \\ X_{I_i} & X_{I_d} \end{bmatrix}\begin{bmatrix} K_i \\ K_d \end{bmatrix}=\begin{bmatrix} 0-X_{R_p}\overline{K_p} \\ -\omega-X_{I_p}\overline{K_p} \end{bmatrix} \tag{35}$$

Although the coefficient matrix is singular, a solution will exist in two cases. First, at $\omega=0$, $K_d(0,\theta_A,\gamma)$ is arbitrary and $K_i(0,\theta_A,\gamma)=0$, unless $\mathrm{Im}(0)=\mathrm{Re}(0)=0$, which holds only when the plant has a zero at the origin. In such a case, a PID controller should be avoided as PID pole will cancel the zero and cause the system to become internally unstable.

A second set of solution will exist for $\omega=\omega_i$, where $K_p(\omega_i,\theta_A,\gamma)=\overline{K_p}$(constant) from equation (24). At these frequencies, $K_d(\omega_i,\theta_A,\gamma)$ and $K_i(\omega_i,\theta_A,\gamma)$ must satisfy the following straight line equation,

$$K_d(\omega_i,\theta_A,\gamma)=\frac{K_i(\omega_i,\theta_A,\gamma)}{\omega_i^{\,2}}+\frac{\mathrm{Im}(\omega_i)+\frac{1}{\gamma}(A_A\sin\theta_A+B_A\cos\theta_A)}{\omega_i X(\omega_i)} \tag{36}$$

3.4 PI controller design in (K_p, K_i) plane

The boundary for $P(\omega, \theta_A, \gamma) = 0$ for the (K_p, K_i) plane for a fixed value of $K_d = \overline{K_d}$ is as explained in Section 3.1. For $K_d = 0$, the PID controller will reduce to the PI controller which is given in the frequency domain by

$$K(j\omega) = K_p + \frac{K_i}{j\omega} \tag{37}$$

where K_p and K_i are the proportional and integral gains of the PI controller, respectively.

The frequency domain representation of the PI controller for $P(\omega, \theta_A, \gamma) = 0$ in the (K_p, K_i) plane is,

$$\begin{bmatrix} X_{R_p} & X_{R_i} \\ X_{I_p} & X_{I_i} \end{bmatrix} \begin{bmatrix} K_p \\ K_i \end{bmatrix} = \begin{bmatrix} 0 \\ -\omega \end{bmatrix} \tag{38}$$

Solving equation (38) for all $\omega \neq 0$ and $\theta_A \in 0, 2\pi$ we obtain,

$$K_p(\omega, \theta_A, \gamma) = \frac{-\mathrm{Re}(\omega) - \frac{1}{\gamma}(A_A \cos\theta_A - B_A \sin\theta_A)}{X(\omega)} \tag{39}$$

$$K_I(\omega, \theta_A, \gamma) = \frac{-\omega\left(\mathrm{Im}(\omega) + \frac{1}{\gamma}(A_A \sin\theta_A + B_A \cos\theta_A)\right)}{X(\omega)} \tag{40}$$

where

$$X(\omega) = \left|G_p(j\omega)\right|^2 + \frac{1}{\gamma^2}\left|W_A(j\omega)\right|^2 + \frac{2}{\gamma}\begin{pmatrix} \mathrm{Re}(\omega)(A_A \cos\theta_A - B_A \sin\theta_A) \\ +\mathrm{Im}(\omega)(A_A \sin\theta_A + B_A \cos\theta_A) \end{pmatrix}$$

For $\omega = 0,$ equation (38) will result in,

$$\begin{bmatrix} 0 & X_{R_i}(0) \\ 0 & X_{I_i} \quad 0 \end{bmatrix} \begin{bmatrix} K_p \\ K_i \end{bmatrix} = \begin{bmatrix} 0 \\ 0 \end{bmatrix} \tag{41}$$

From equation (41) it can be concluded that $K_p(0,\theta_A,\gamma)$ is arbitrary and $K_i(0,\theta_A,\gamma) = 0,$ unless $X_{R_i}(0) = X_{I_i}(0) = 0$ which is possible only when $\gamma \to \infty$ and $R_p(0) = I_p(0) = 0,$ which holds only when $G_p(s)$ has a zero at the origin.

CHAPTER 4

EXAMPLES

4.1 PID controller design for a DC motor with time-delay.

In this section, we seek to control a DC motor model with a communication time-delay, as shown in Figure 16 where $G(s)$ is the DC motor, $K(s)$ is the PID controller, and $e^{-\tau s}$ represents the τ second communication time-delay.

4.1.1. Design goal

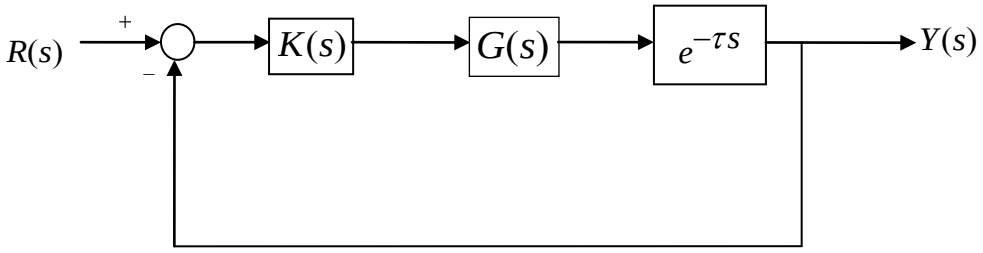

Figure 16. DC motor model with time delay

The design goal is to find the set of PID controllers that will guarantee that the robust stability constraint,

$$\left\| W_A(j\omega)K(j\omega)S(j\omega) \right\|_\infty \le \gamma \tag{42}$$

is satisfied for $\gamma = 1$, thereby ensuring nominal and robust stability for the perturbed plant. Here $W_A(j\omega)$, $K(j\omega)$, and $S(j\omega)$ are the additive uncertainty weight, PID controller, and sensitivity function given in equation (13).

4.1.2. Plant model

The transfer function model of a DC motor can be represented as

$$G(s) = \frac{65.5}{s(s+34.6)} \tag{43}$$

In this thesis, the range of the unknown communication time-delay is

$$\tau \in [0.05, 0.15] \tag{44}$$

The nominal model of the DC motor for controller design is chosen to be

$$G_p(s) = \frac{65.5}{s(s+34.6)} e^{-\bar{\tau}s} \tag{45}$$

where τ is selected to be the mean value of the time delay range, i.e., $\bar{\tau} = 0.1$.

4.1.3. Designing additive uncertainty weight

As discussed in Section 2.5.1, the parametric and unmodelled dynamics uncertainty can be combined into a single lumped perturbation of a chosen structure. Here, an additive uncertainty structure is considered in order to bound the range of uncertainties present in the plant.

Figure 17 represents a basic additive uncertainty structure used for the uncertain model [4].

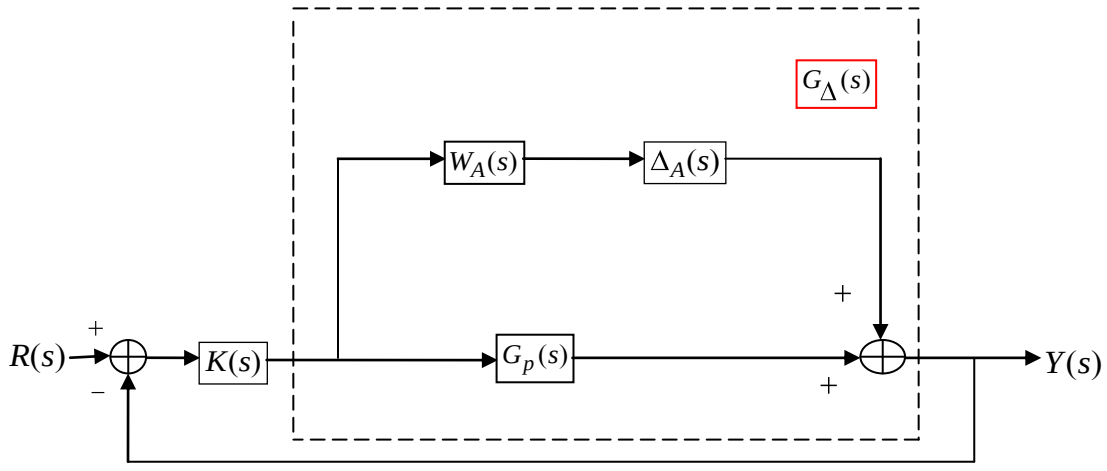

Figure 17. Additive uncertainty representation for D.C. motor with time delay.

The uncertain DC motor model is represented as

$$G_{\Delta}(s) = G_{P}(s) + W_{A}(s)\Delta_{A}(s) \tag{46}$$

where $\Delta_{A}(s)$ is any stable transfer function such that $\forall \omega$ [4],

$$\left|\Delta_{A}(j\omega)\right| \leq 1 \tag{47}$$

where

$$\left|\Delta_{A}(j\omega)\right| = \left|\frac{G_{\Delta}(j\omega) - G(j\omega)}{W_{A}(j\omega)}\right| \tag{48}$$

Combining equation (47) and equation (48) we obtain,

$$\left|\frac{G_{\Delta}(j\omega) - G_{p}(j\omega)}{W_{A}(j\omega)}\right| \leq 1, \forall \omega \tag{49}$$

Therefore in order to cover the entire uncertainty set, it is required to find an additive uncertainty weight $W_{A}(s),$ such that

$$\left|W_{A}(j\omega)\right| \geq \left|G_{\Delta}(j\omega) - G_{p}(j\omega)\right| \tag{50}$$

where $$\left|G_{\Delta}(j\omega) - G_{p}(j\omega)\right| = \left|\frac{65.5}{j\omega(j\omega + 34.6)}\right|\left|e^{-\tau\ j\omega} - e^{-\bar{\tau}\ j\omega}\right|$$

i.e., the additive uncertainty weight is designed such that,

$$\left|W_{A}(j\omega)\right| \geq \left|\frac{65.5}{j\omega(j\omega + 34.6)}\right|\left|e^{-j\ \tau\omega} - e^{-j\ \bar{\tau}\omega}\right| \tag{51}$$

The following form was selected for the weight,

$$W_{A}(s) = \frac{M_{h}}{(s/\omega_{c_1} + 1)(s/\omega_{c_2} + 1)} \tag{52}$$

The additive weight transfer function obtained was,

$$W_A(s) = \frac{0.13}{(s/20.67+1)(s/100+1)} \tag{53}$$

Figure 18 shows the additive uncertainty weight that bounds the entire uncertainty set.

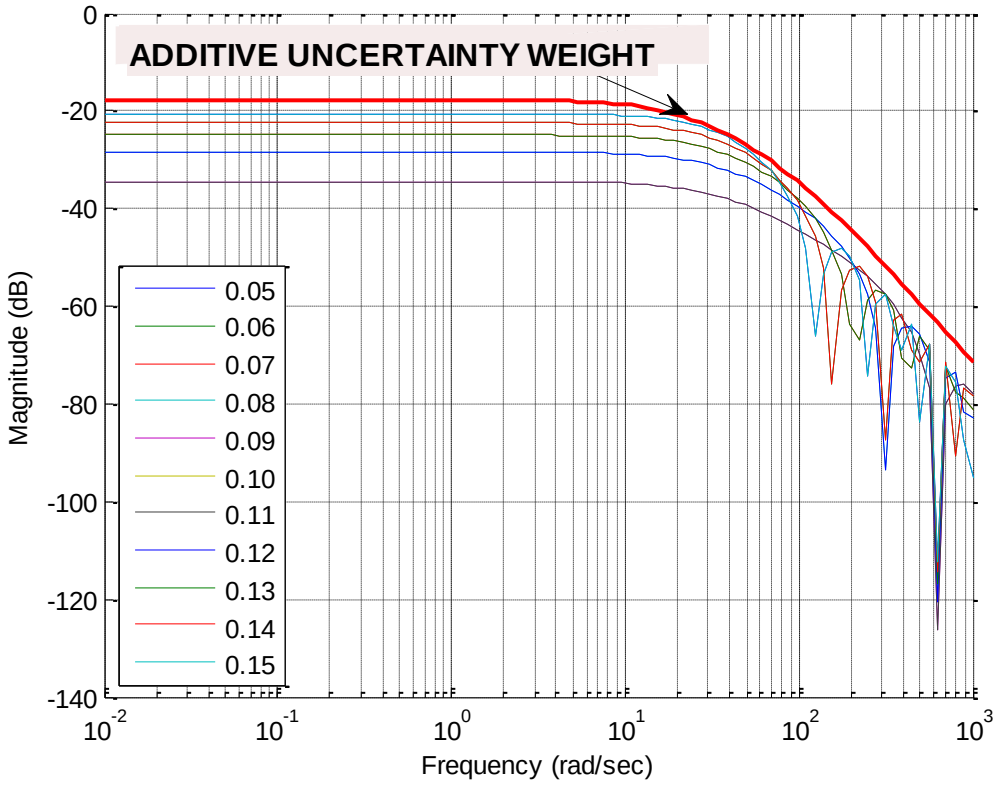

Figure 18. Additive weight representation

4.1.4. Finding all PID controllers in (K_p, K_i) plane for a constant value of K_d

In this section, using the design methodology explained in Section 3.1, we will determine the set of PID controllers that will ensure robust stability in the (K_p, K_i) plane for a constant value of K_d. The DC motor model $G(s)$ is as presented in equation (43). As explained in Section 3.1, for a constant value of K_d, it is possible to obtain the entire set of PID controllers at the boundary of $P(\omega, \theta_A, \gamma) = 0$ in the (K_p, K_i) plane. In this example, we have considered $\overline{K_d} = 0.2$.

Using equation (24) and equation (25), the nominal stability boundary and robust stability region are obtained in the (K_p, K_i) plane. As discussed in chapter 3, the PID nominal stability boundary of the plant can be obtained by setting $\gamma \to \infty$. PID controllers that satisfy the robust stability constraint in equation (42) are found by setting $\gamma = 1$ and then finding the intersection of all regions for $\theta_A \in (0, 2\pi)$. The region that satisfies the robust stability constraint and the nominal stability boundary in the (K_p, K_i) plane for $K_d = 0.2$ is as shown in Figure 19. The intersection of all regions inside the nominal stability boundary of the (K_p, K_i) is the robust stability region.

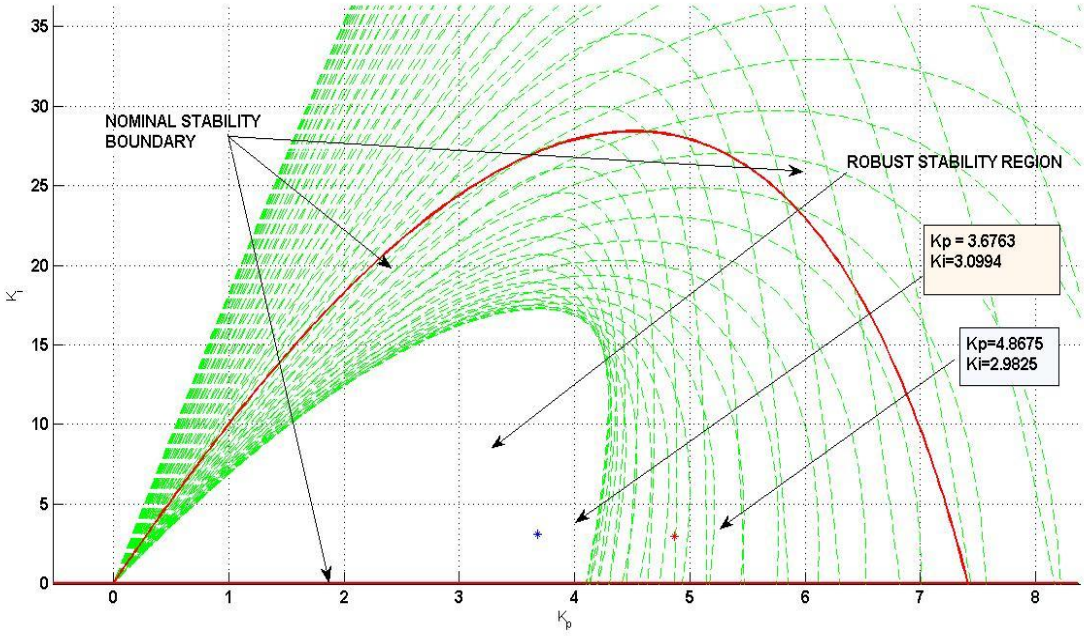

Figure 19. Nominal stability boundary and robust stability region for K_p and K_i values (K_d=0.2)

To check our results, a PID controller, $K_1(s)$, is selected from the robust stability region and another PID controller, $K_2(s)$, is selected from outside this region.

$$K_1(s) = 3.6763 + \frac{3.0994}{s} + 0.2s \tag{54}$$

$$K_2(s) = 4.8675 + \frac{2.9825}{s} + 0.2s \tag{55}$$

Substituting equation (54) and equation (53) into equation (42) gives $\|W_A(j\omega)K_1(j\omega)S(j\omega)\|_\infty = 0.8289$. Repeating this process for equation (55) and equation (53) results in $\|W_A(j\omega)K_2(j\omega)S(j\omega)\|_\infty > 1$. Figure 20 shows the Bode plot for $\|W_A(j\omega)K_i(j\omega)S(j\omega)\|$ for PID controllers $K_1(s)$ and $K_2(s)$ selected from the (K_p, K_i) plane.

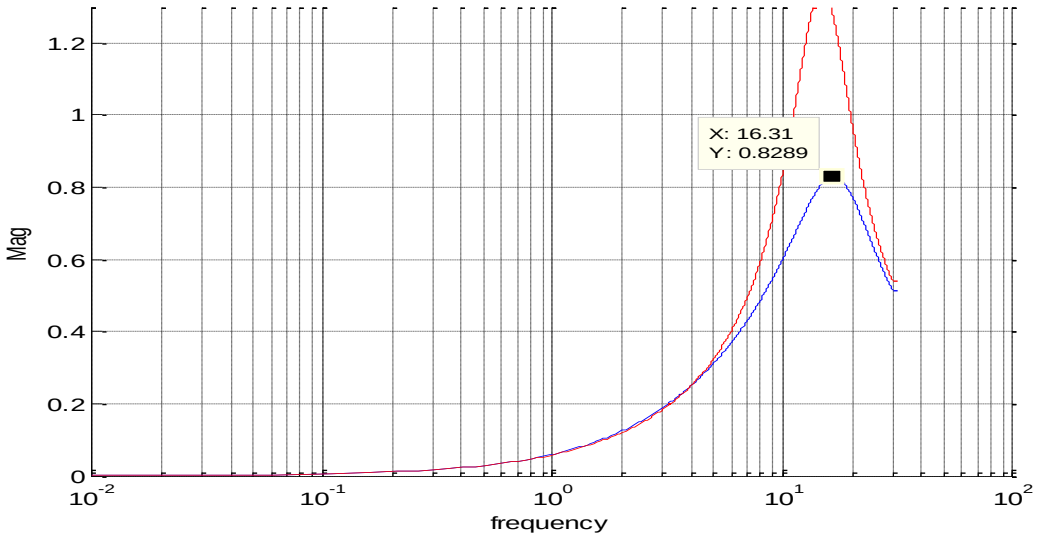

Figure 20. Magnitude of $W_A(j\omega)K_i(j\omega)S(j\omega)$ for

$K_1(s) = 3.6763 + \frac{3.0994}{s} + 0.2s$ and $K_2(s) = 4.8675 + \frac{2.9825}{s} + 0.2s$

Thus, the PID controller selected from the robust stability region clearly satisfies the robust stability constraint while the other does not. After repeated simulations done in MATLAB it can be concluded that any controller selected from inside the robust stability region will enable robust stability for the perturbed system. Thus, the design goal is met in this plane.

4.1.5. Finding all PID controllers in (K_p, K_d) plane for a constant value of K_i

In this section, using the design methodology explained in Section 3.2, we will determine the set of PID controllers that will ensure robust stability in the (K_p, K_d) plane for a constant value of K_i. The DC motor model $G(s)$ is as presented in equation (43). As explained in Section 3.2, for a constant value of K_i, it is possible to obtain the entire set of PID controllers at the boundary of $P(\omega, \theta_A, \gamma) = 0$ in the (K_p, K_d) plane. In this example, we have considered $K_i = 1$.

Using equation (29) and equation (30) in MATLAB, the nominal stability boundary and robust stability region are obtained in the (K_p, K_d) plane. As discussed in chapter 3, the PID nominal stability boundary of the plant can be obtained by setting $\gamma \to \infty$. PID controllers that satisfy the robust stability constraint in equation (42) are found by setting $\gamma = 1$ and then finding the intersection of all regions for $\theta_A \in (0, 2\pi)$. The region that satisfies the robust stability constraint and the nominal stability boundary in the (K_p, K_d) plane for $K_i = 1$ is as shown in Figure 21.

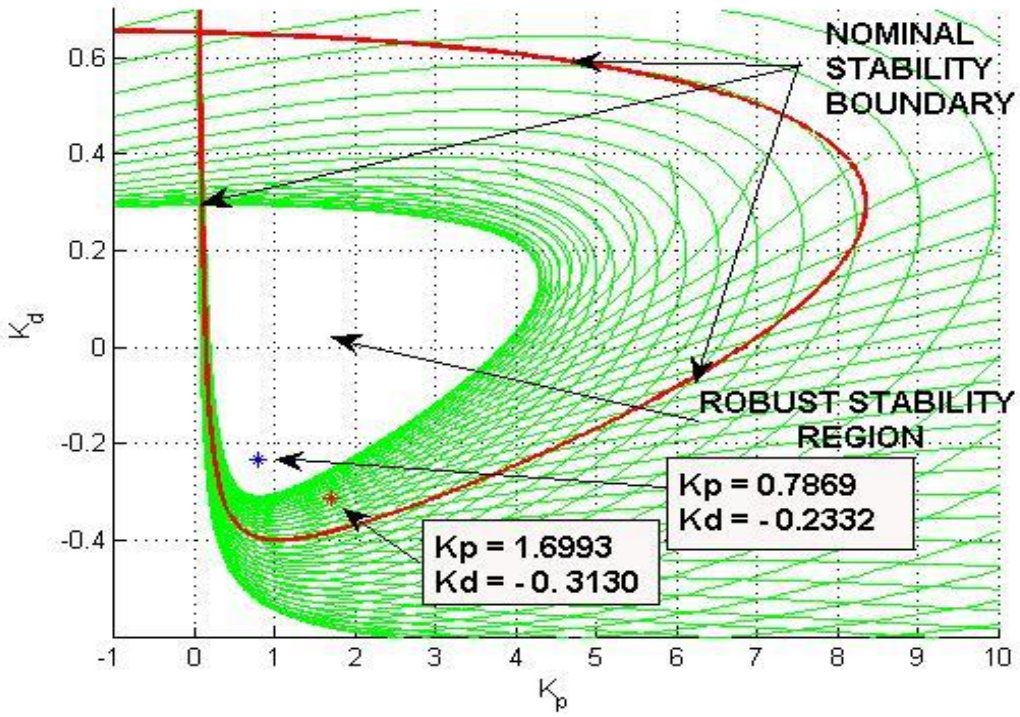

Figure 21. Nominal stability boundary and robust stability region
for K_p and K_d values $(K_i = 1)$

The intersection of all regions inside the nominal stability boundary is the robust stability region in the (K_p, K_d) plane. To verify the results, a PID controller, $K_1(s)$ is selected from the robust stability region and another PID controller, $K_2(s)$, is selected from outside this region

$$K_1(s) = 0.7869 + \frac{1}{s} - 0.2332s \tag{56}$$

$$K_2(s) = 1.6993 + \frac{1}{s} - 0.3130s \tag{57}$$

Substituing equation (56) and equation (53) into equation (42) gives $\|W_A(j\omega)K_1(j\omega)S(j\omega)\|_\infty = 0.4606$. Repeating this process for equation (57) and equation (53)

results in $\left\|W_A(j\omega)K_2(j\omega)S(j\omega)\right\|_\infty > 1$. This clearly implies that the PID controller selected from the robust stability region satisfies the robust stability constraint, while the other does not.

Figure 22 shows the Bode plot for $\left|W_A(j\omega)K_i(j\omega)S(j\omega)\right|$ for PID controllers $K_1(s)$ and $K_2(s)$ selected from the (K_p, K_d) plane.

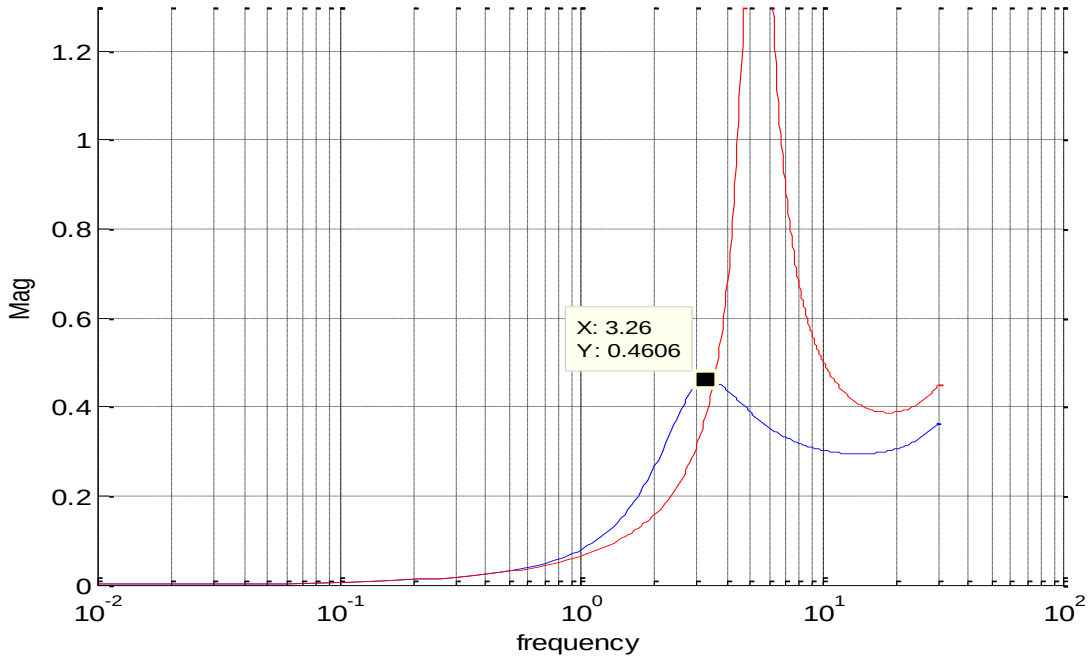

Figure 22. Magnitude of $W_A(j\omega)K_i(j\omega)S(j\omega)$

for $K_1(s) = 0.7869 + \frac{1}{s} - 0.2332s$ and $K_2(s) = 1.6993 + \frac{1}{s} - 0.3130s$.

4.1.6. Finding all PID controllers in (K_i, K_d) plane for a constant value of K_p

The primary goal in this section is to find all PID controllers that will ensure robust stability in the (K_i, K_d) plane for a constant value of $K_p = \overline{K_p}$. As discussed in Section 3.3, the coefficient matrix being singular, a solution will exist at $\omega = 0$, where $K_d(0, \theta_A, \gamma)$ is arbitrary and $K_i(0, \theta_A, \gamma) = 0$ if and only if $\mathrm{Im}(0) = \mathrm{Re}(0) = 0$, which holds only when the plant has a

zero at the origin. In such a case, a PID compensator should be avoided as PID pole will cancel the zero and the system becomes internally unstable.

The second set of solution will exist for $\omega = \omega_i$, where $K_p(\omega_i, \theta_A, \gamma) = \overline{K_p}$. At these frequencies, $K_i(\omega_i, \theta_A, \gamma)$ and $K_d\ \omega_i, \theta_A, \gamma$ must satisfy the straight line equation given in equation (36). In our MATLAB simulation we have considered, $\overline{K_p} = 0.5$. Figure 23 represents the range of ω_i obtained for $\overline{K_p} = 0.5$.

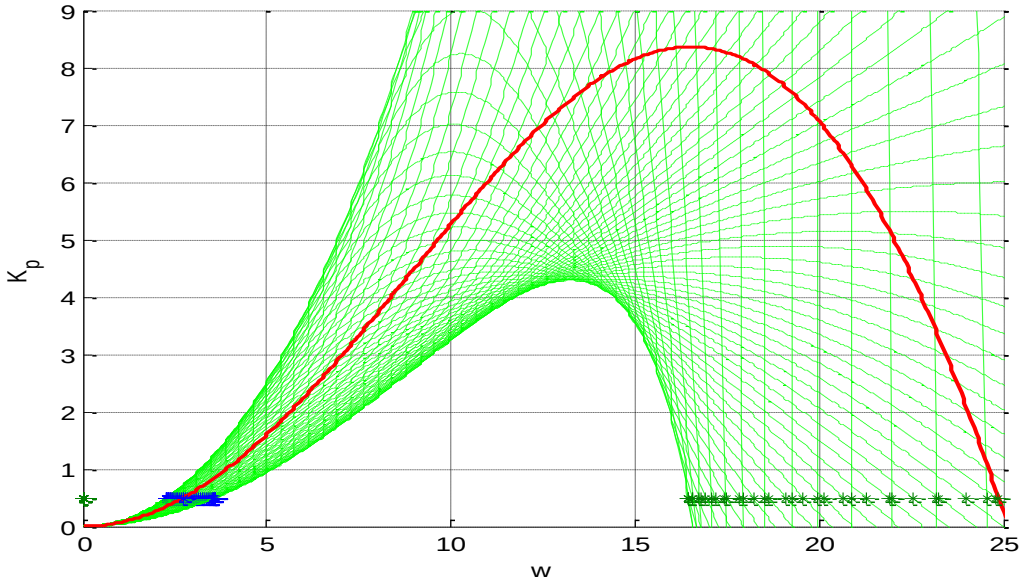

Figure 23. Range of frequencies (ω_i) for constant value of $K_p = 0.5$

We can now obtain the entire range of PID gains in the (K_i, K_d) plane for $\omega = \omega_i$ such that they satisfy the straight line equation (36). The nominal stability boundary and the robust stability region in the (K_i, K_d) plane for a $K_p = 0.5$ are shown in Figure 24.

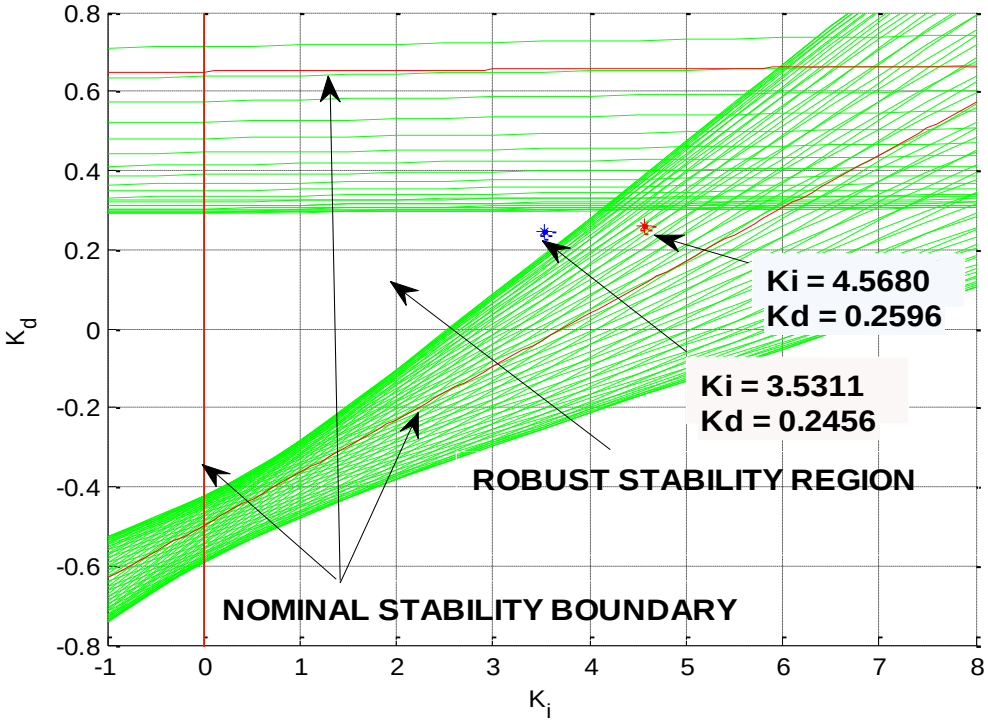

Figure 24. Nominal stability boundary and robust stability region for K_i and K_d values for $K_p = 0.5$

To verify the results, a PID controller, $K_1(s)$, is selected from the robust stability region and another PID controller, $K_2(s)$, is selected from outside this region.

$$K_1(s) = 0.5 + \frac{3.5311}{s} + 0.2456s \tag{58}$$

$$K_2(s) = 0.5 + \frac{4.5680}{s} + 0.2596s \tag{59}$$

Substituing equation (58) and equation (53) into equation (42) gives $\left\|W_A(j\omega)K_1(j\omega)S(j\omega)\right\|_\infty = 0.78$. Repeating this process for equation (59) and equation (53) results in $\left\|W_A(j\omega)K_2(j\omega)S(j\omega)\right\|_\infty > 1$. This clearly implies that the PID controller selected from the robust stability region satisfies the robust stability constraint, while the other does not.

Figure 25 shows the Bode plot for $\left|W_A(j\omega)K_i(j\omega)S(j\omega)\right|$ for PID controllers $K_1(s)$ and $K_2(s)$ selected from the (K_i, K_d) plane.

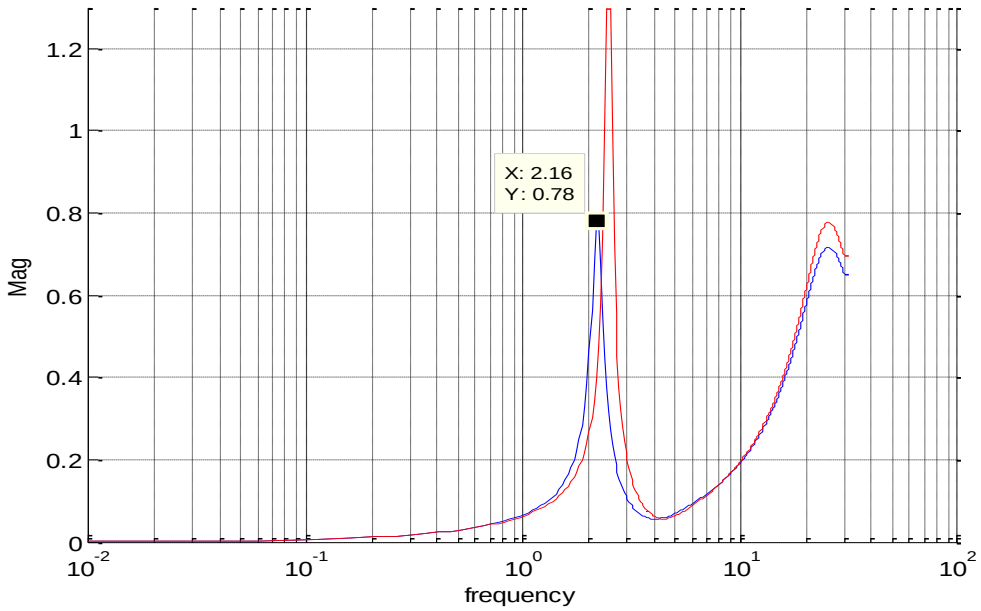

Figure 25. Magnitude of $W_A(j\omega)K_i(j\omega)S(j\omega)$ for

$K_1(s) = 0.5 + \frac{3.5311}{s} + 0.2456s$ and $K_2(s) = 0.5 + \frac{4.5680}{s} + 0.2596s$.

4.1.7 Conclusion

In this section, a graphical design method for obtaining all PID controllers that will satisfy a robust stability constraint for a DC motor with time delay were discussed. Observing the results in Sections 4.1.4, 4.1.5, and 4.1.6, it can be concluded that the PID controllers selected from the robust stability regions in the (K_p, K_i), (K_p, K_d), and (K_i, K_d) planes satisfy the robust stability constraint for the DC motor model.

4.2. PI controller design for a single area non-reheat steam generation unit with additive uncertainty

As discussed in Section 2.9, the sheer cost involved in the entire power system operation process demands a robust and stable control system that will ensure the smooth operation of power flow from the generating stations to the consumers. The interconnected grid system which allows power to be transferred from one control area to another, is extremely complicated. The grid-system breakdown that occurred on November 9, 1965 on the east coast of North America, when an automatic control device that regulates and directs current flow failed in Queenstown, Ontario, caused a circuit breaker to remain open, is a perfect example of the vulnerability of this system. Therefore, a robust control structure to minimize these situations is of high priority.

As mentioned in Section 2.7, frequent load and generation mismatch tends to drive the system frequency from its nominal value. In [2], the author has mentioned how in real LFC systems, PI controllers play a major role. However, the lack of a satisfactory method for tuning the PI controller parameters leads to an inability to obtain good performance for various operating conditions and frequent load changes in a multi-area power system. The presence of uncertainties like system restructuring and changes in dynamic/load and operating conditions has led to a uncertainties being a serious issue in power system operation [2]. All these factors reflect the necessity of a controller design method that will do a better job of tuning the controllers involved and that will robustly stabilize the control areas .

In this section, our graphical design method is implemented to obtain all PI controller gains that will robustly stabilize a single-area non-reheat steam generator unit. For simulation purpose, we have assumed ±20% parametric uncertainty present in the governor and rotating mass and load model.

4.2.1. Design goal

Our goal is to determine the range of PI controllers that will guarantee that the robust stability constraint

$$\left\| W_A(j\omega)K(j\omega)S(j\omega) \right\|_\infty \leq 1 \tag{60}$$

is satisfied where $W_A(j\omega)$, $K(j\omega)$, and $S(j\omega)$ are the additive uncertainty weight, PI controller, and sensitivity function from equation (13). If equation (60) is satisfied then it can be confirmed that the selected controllers are capable of robustly stabilizing the perturbed system.

4.2.2. Plant model

A general block diagram of a non-reheat steam generator unit is shown in Figure 26. In Figure 26, $G_1(s)$, $G_2(s)$ and $G_3(s)$ represent the transfer function models of the primary speed governor, non-reheat steam turbine, and rotating mass and load models, respectively. B_i and R_i are the frequency bias factor and speed-droop characteristics for control area i. T_{ai} and T_{pi} are the total tie-line power interchange for control area i and tie-line power interchange between external control areas.

The PI controller is represented as $K(s)$ where the input to the controller is the Area Control Error (ACE). ΔP_{L_i} is the load change experienced by control area i. ΔP_{c_i}, ΔP_{e_i}, ΔP_{g_i} and ΔP_{m_i} are the supplementary control output, governor input, primary governor output change, and turbine output power change. ΔP_{mech} and Δf_i are the mechanical power input to the rotating mass and load unit and frequency deviation from nominal value, respectively. $2\pi/s$ is the integral gain added to the feedback loop.

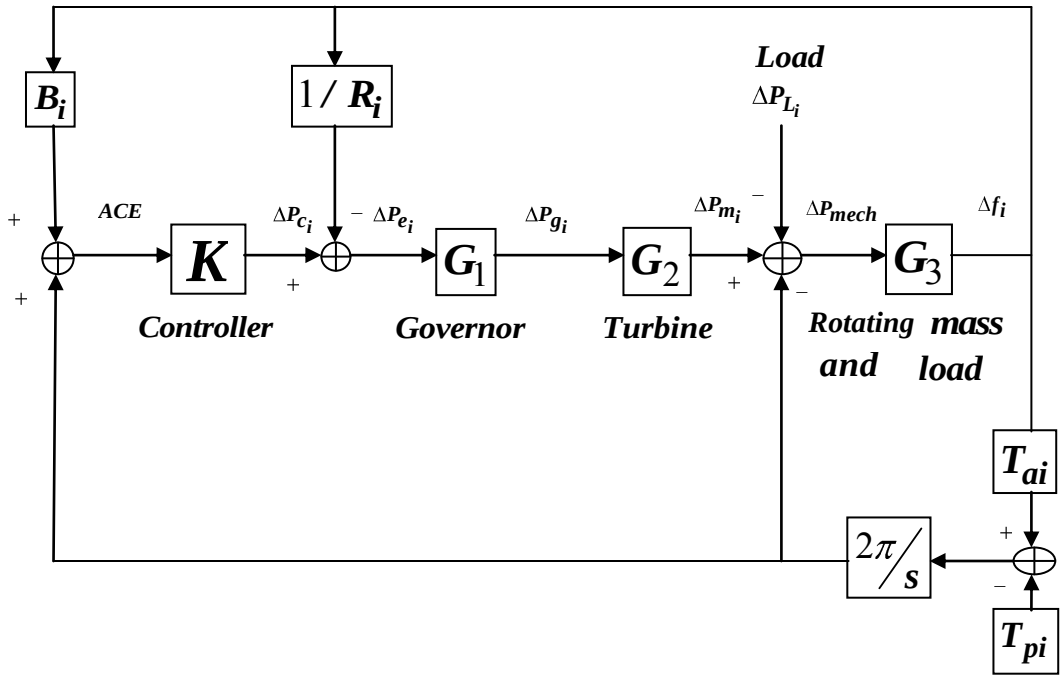

Figure 26. Block diagram representation of a single area non-reheat steam generation unit [2].

A general transfer function model of the speed governor is

$$G_1(s) = \frac{1}{1+sT_{gi}} \tag{61}$$

where T_{gi} is the governor time coefficient. A general transfer function model of the non-reheat steam turbine is given by

$$G_2(s) = \frac{1}{1+sT_{ti}} \tag{62}$$

where T_{ti} is the turbine charging time. A general transfer function model for the rotating mass and load model is

$$G_3(s) = \frac{1}{D_i + M_i s} \tag{63}$$

where D_i and M_i are the load damping and the generator inertia coefficients, respectively. The tie line coefficients are

$$T_{ai} = \sum_{\substack{j=1 \\ j \neq i}}^{N} T_{ij} \tag{64}$$

$$T_{pi} = \sum_{\substack{j=1 \\ j \neq i}}^{N} T_{ij} \Delta f_j \tag{65}$$

Here, T_{ij} is the tie-line synchronizing coefficient of area i with interconnected areas j and Δf_j is the corresponding frequency deviation in area j, respectively [1, 2]. Frequency bias factor (B_i) for control area i is given as,

$$B_i = \frac{1}{R_i} + D_i \tag{66}$$

Figure 27 represents the nominal model $G_p(s)$, of this single area non-reheat generation unit. The closed loop transfer function for this model can be found from the following equations,

$$G_p(s) = G_{p1}(s) + G_{p2}(s) \tag{67}$$

where

$$G_{p1}(s) = \frac{2\pi}{s} T_{ai} G_3(s) G_2(s) G_1(s) \left(\left(1 + \frac{2\pi}{s} G_3(s) T_{ai} \right)^{-1} + \left(1 + \frac{1}{R_i} G_3(s) G_2(s) G_1(s) \right)^{-1} \right) \tag{68}$$

$$G_{p2}(s) = B_i G_3(s) G_2(s) G_1(s) \left(\left(1 + \frac{2\pi}{s} G_3(s) T_{ai} \right)^{-1} + \left(1 + \frac{1}{R_i} G_3(s) G_2(s) G_1(s) \right)^{-1} \right) \quad (69)$$

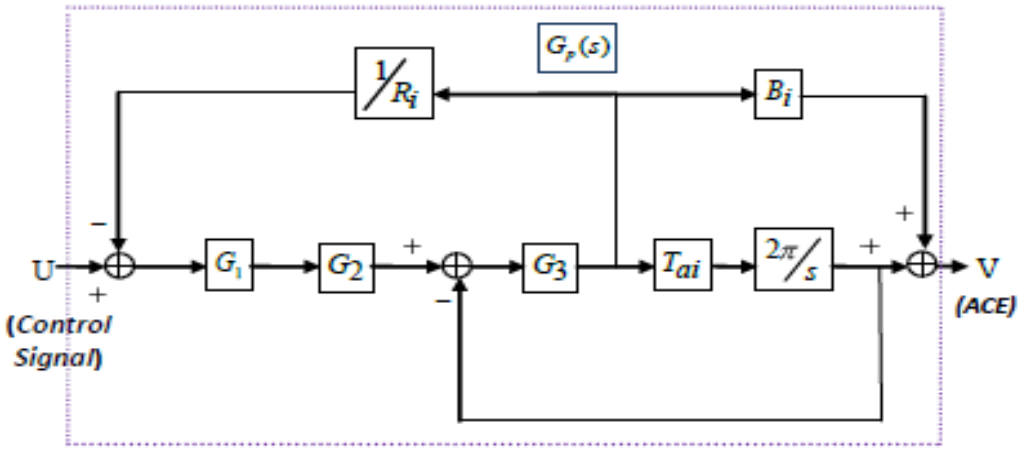

Figure 27. Nominal model of a non-reheat steam generator unit

Substituting equation (69) and equation (70) into equation (68), we obtain the nominal model as,

$$G_p(s) = \left(\frac{2\pi}{s} T_{ai} + B_i \right) G_3 G_2 G_1 \left(\left(1 + \frac{2\pi}{s} G_3 T_{ai} \right)^{-1} + \left(I + \frac{1}{R_i} G_3 G_2 G_1 \right)^{-1} \right) \quad (70)$$

4.2.3. Additive uncertainty weight design

As mentioned in Section 3.4., the boundary for $P(\omega, \theta_A, \gamma) = 0$ for the (K_p, K_i) plane for $K_d = 0$ generates a PI controller as,

$$K(j\omega) = K_p + \frac{K_i}{j\omega} \quad (71)$$

In order to analyze robust stability for our designed controller we have assumed ±20% uncertainty in the plant parameters. This is shown in Table 2.

TABLE 2.
UNCERTAIN PARAMETERS

Plant parameter	**Uncertainty Range**
Governor Time coefficient, T_{g1}	[0.064,0.096]
Load-damping coefficient, D_1	[0.012,0.018]
Rotor Inertia coefficient, M_1	[0.133,0.199]

The nominal plant parameters for the single unit non-reheat generator unit are as referenced in [2]. In [2] these parameters were used to obtain the dynamic response of a closed loop steam generation unit for a step load disturbance of 0.02 per unit. The nominal parameter values are as shown in Table 3. In this thesis, the results obtained by using these parameters were satisfactory as the robust stability constraint was satisfied.

TABLE 3
NOMINAL PLANT PARAMETERS

Plant Parameter	**Value**	**Per unit measure**
$D_1\left(=\frac{\Delta P_l}{\Delta\omega}\right)$	0.015	pu/Hz
$M_1 = \omega I$	0.1667	pu s
$R_1\left(=\frac{\Delta\omega}{\Delta P}\right)$	3.00	Hz/pu
T_{g1}	0.08	s

TABLE 3 (continued)

Plant Parameter	Value	Per unit measure
T_{t1}	0.40	s
T_{a1}	0.45	pu/Hz
$B_1\left(=1/R_1+D_1\right)$	0.3483	pu/Hz

The additive weight transfer function is selected as,

$$\left|W_A(j\omega)\right| \geq \left|G_\Delta(j\omega) - G_p(j\omega)\right| \tag{72}$$

where $G_\Delta(s)$ represents the uncertain plant and $\left|G_\Delta(j\omega) - G_p(j\omega)\right|$ is the peak magnitude of the worst case uncertain plant such that

$$G_\Delta = ((\frac{2\pi}{s}T_{a1} + B1) * G_{31} * G_2 * G_{11} * (Go1 + Go)) \tag{73}$$

where *Go1* represent the feedback loop which includes $\frac{2\pi}{s}$ and T_{a1}, *Go* represent the feedback loop which includes $\frac{1}{R_1}$. G_{31} represent the worst case uncertainty rotating mass-load model, G_{11} represent the worst case uncertainty governor model. In this example, the worst case uncertainties are obtained for $T_{g1} = 0.064,\ M_1 = 0.133,$ and $D_1 = 0.012.$

Selecting the additive weight transfer function to bound the entire range of plant uncertainties give us

$$W_A(s)=\frac{\left\{\begin{array}{l}2.9(10E-9)s^{15}+1.3(10E-7)s^{14}+2.5(10E-6)s^{13}+2.6(10E-5)s^{12}+\\1.78(10E-4)s^{11}+9.2(10E-4)s^{10}+3.8(10E-3)s^{9}++0.011s^{8}+0.029s^{7}+0.056s^{6}\\+0.079s^{5}+0.077s^{4}+0.04s^{3}+0.005s^{2}+0.0002s\end{array}\right\}}{\left\{\begin{array}{l}4.9(10E-11)s^{18}+2.9(10E-9)s^{17}+7.3(10E-8)s^{16}+9.96(10E-7)s^{15}+\\8.87(10E-6)s^{14}+5.95(10E-5)s^{13}+3.2(10E-4)s^{12}+1.3(10E-3)s^{11}+\\4.9(10E-3)s^{10}+0.01s^{9}+0.032s^{8}+0.057s^{7}+0.07s^{6}+0.068s^{5}+\\0.03s^{4}+0.005s^{3}+0.0002s^{2}\end{array}\right\}} \quad (74)$$

This is shown in Figure 28.

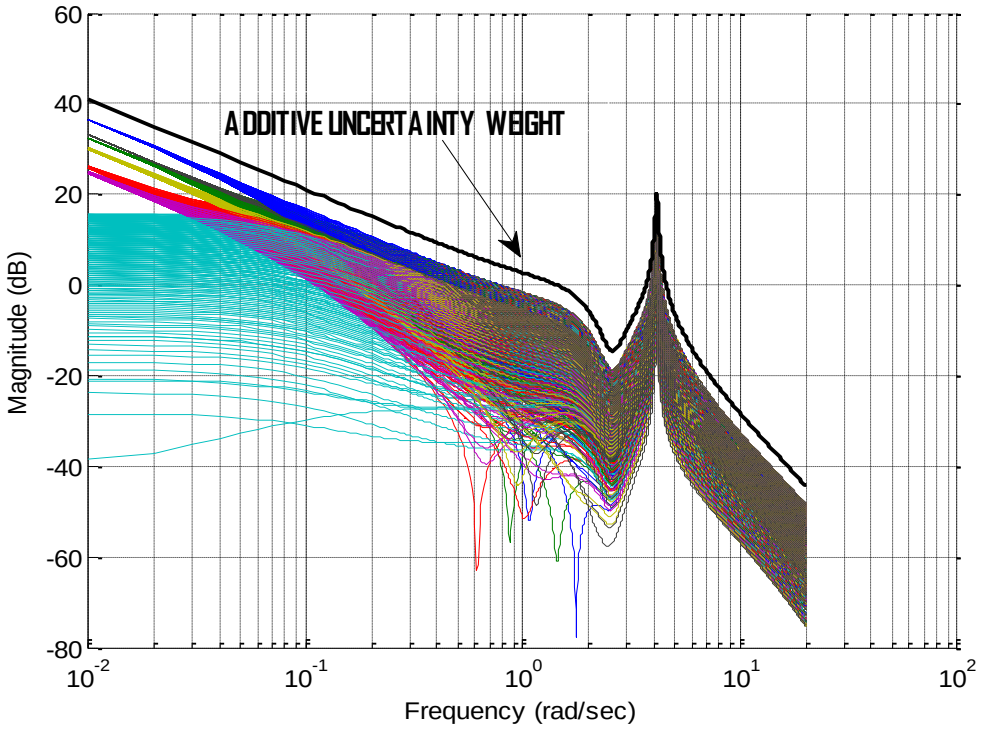

Figure 28. Additive uncertainty weight for single- area steam generator unit.

4.2.4. PI controller design

From equation (70), the nominal plant transfer function is

$$G_p(s) = \frac{5.1\ (10E-2\ \ s^6 + 1.17s^5 + 7.79s^4 + 18.7s^3 + 49.5s^2 + 48s + 3.9}{\left\{\begin{array}{l} 7.4(10E-4)s^9 + 2.1(10E-2)s^8 + 2.1(10E-1)s^7 + 9.9(10E-1)s^6 + \\ 4.5s^5 + 11.5s^4 + 18.8s^3 + 18.0s^2 + 1.5s \end{array}\right\}} \qquad (75)$$

By substituting the frequency response of the transfer function models $W_A(s)$ and $G_p(s)$ into equation (39) and equation (40), we can now obtain the entire range of PI gains in the (K_p, K_i) that satisfy the robust stability given in equation (60). The region that satisfies the robust stability constraint and the nominal stability boundary in the (K_p, K_i) plane for the single area non-reheat steam generator unit is shown in Figure 29.

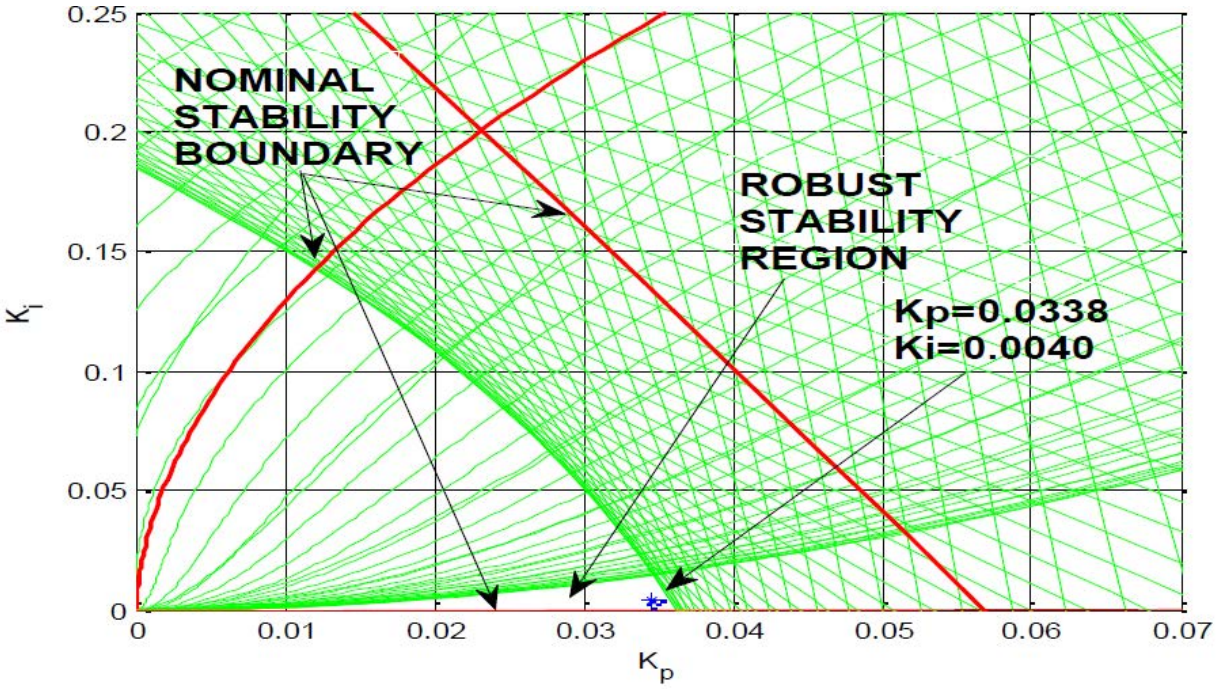

Figure 29. Nominal stability boundary and robust stability region for the single area generator unit (±20% uncertainty) in (K_p, K_i) plane.

In order to verify the results, an arbitrary PI controller is selected from the robust stability region as

$$K(s) = 0.0338 + \frac{0.0040}{s} \tag{76}$$

Substituting equation (74), equation (75), and equation (76) into equation (60) results in, $\left\| W_A(j\omega)K(j\omega)S(j\omega) \right\|_\infty = 0.8138.$ This confirms that the PI controllers selected from our designed robust stability region satisfy the robust stability constraint. The Bode plot representation of $\left| W_A(j\omega)K(j\omega)S(j\omega) \right|$ is as shown in Figure 30.

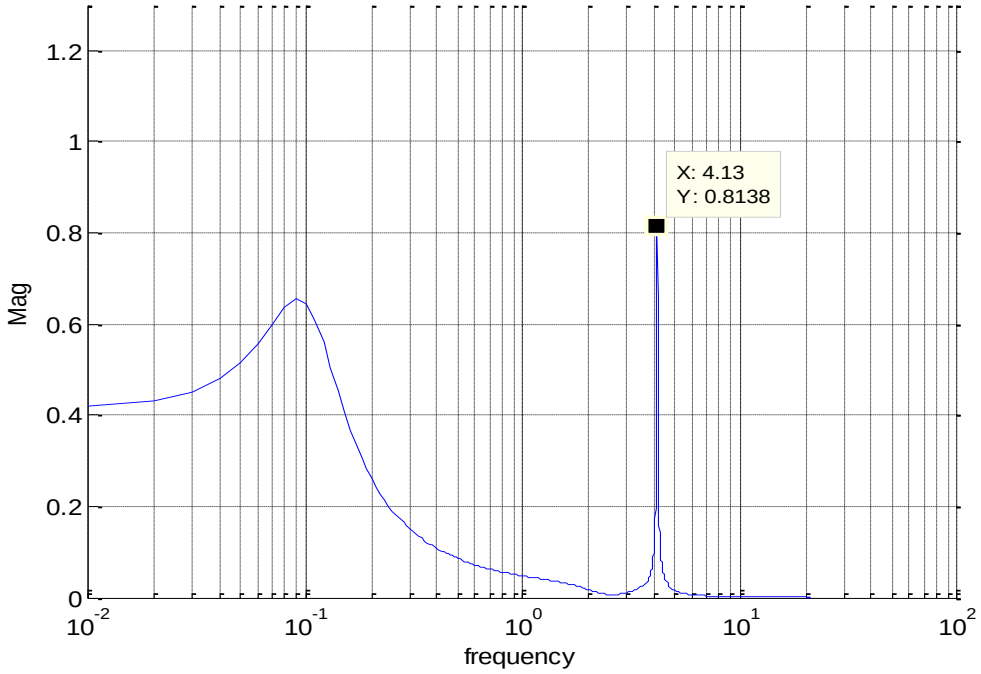

Figure 30. Magnitude of $W_A(j\omega)K(j\omega)S(j\omega)$ for

$$K(s) = 0.0338 + \frac{0.0040}{s}$$

4.2.5. Conclusion

In this section, a graphical design method for obtaining all PI controllers that will satisfy a robust stability constraint for a non-reheat steam generator unit was presented. The additive uncertainty modeling technique was used to obtain an additive weight that bounds the entire uncertainty set.

CHAPTER 5

CONCLUSION AND FUTURE WORK

5.1 Conclusion

In this thesis, a graphical design method was introduced for finding all achievable PI/PID compensators that will ensure nominal stability and robust stability for any arbitrary order SISO LTI plant with additive uncertainty. This compensator design method may reduce the complexities involved in plant modeling as it is based on the frequency response of the plant rather than the plant transfer function coefficients.

A cascade DC motor model with time delay and a single area non-reheat steam generator unit are studied to demonstrate the application of this design method. AGC and its role in power generation control is also discussed. The results were satisfactory as the weighted sensitivity constraints were satisfied for our selected PID/PI compensators.

5.2 Future Research

This graphical design method is capable of ensuring closed loop stability for arbitrary order plants with additive uncertainty, which makes is applicable for wide range of plants. Future research can be done in the area of controller design for multi-area power system generation control, multivariable feedback control systems, and robust performance for arbitrary order plants with additive uncertainty.

REFERENCES

LIST OF REFERENCES

[1] Wood, A.J. and B.F. Wollenberg, *Power Generation, Operation, and Control*, 2nd ed., Wiley India (P.) Ltd., 4435/7, Ansari Road, Daryaganj, New Delhi 110 002, India, 2007, Chapter 9, pp. 328-360.

[2] H. Bevrani, *Robust Power System Frequency Control*, Springer Science + Business Media, LLC, 233 Spring Street, New York, NY-10013, USA, 2009, Chapter 2, pp.15-30.

[3] Dorf, Richard C. and Robert H. Bishop, *Modern Control Systems*, 9th ed., Prentice–Hall Inc., New Jersey-07458, USA, 2001, Chapters 1, 5, pp. 1-23, pp. 173-206.

[4] Skogestad, S. and I. Postlethwaite, *Multivariable Feedback Control*, John Wiley & Sons Ltd., Baffins lane, Chicester, West Sussex PO19 1UD, England, 2001, Chapters 2, 7, pp. 15-62, pp. 253-290.

[5] Bhattacharyya, S.P., Chapellat, H., and L.H. Keel, *Robust Control: The Parametric Approach*, Prentice Hall, N.J., 1995.

[6] Ho., K.W., Datta, A., and S.P. Bhattacharya, "Generalizations of the Hermite-Biehler theorem," *Linear Algebra and its Applications*, Vol. 302-303, 1999, pp. 135-153.

[7] Ho., K.W., Datta, A., and S.P. Bhattacharya, "PID stabilization of LTI plants with time-delay," *Proc. 42nd IEEE Conf. on Decision and Control*, Maui, Hawaii, 2003.

[8] Bhattacharyya, S.P. and L.H. Keel, "PID controller synthesis free of analytical methods," *Proc. of IFAC 16th Triennial World Congress*, Prague, Czech Republic, 2005.

[9] Sujoldzic, S. and J.M. Watkins, "Stabilization of an arbitrary order transfer function with time delay using PI and PD controllers," *Proc. of American Control Conference*, June 2006, pp. 2427-2432.

LIST OF REFERENCES (continued)

[10] Sujoldzic S. and J.M. Watkins, "Stabilization of an arbitrary order transfer function with time delay using PID controller," *Proc. of IEEE Conf. on Decision and Control,* Vol. 45, December 2005.

[11] Emami, T. and J.M. Watkins, "Weighted sensitivity design of PID controllers for arbitrary-order transfer functions with time-delay," *Proc. of the IASTED International Conf. on Intelligent Systems and Control*, November 2008, pp 20-25.

[12] Emami, T. and J.M. Watkins, "Robust stability design of PID controllers for arbitrary-order transfer functions with uncertain time delay," *Southeastern Symposium on System Theory University of Tennessee Space Institute*, March 2009, pp. 184-189.

[13] Emami, T. and J.M. Watkins, "Complementary sensitivity design of PID controllers for arbitrary-order transfer functions with time delay," *Proc. of 2008 ASME Dynamic Systems and Control Conf.*, October 2008.

[14] Emami, T. and J.M. Watkins, "Robust performance characterization of PID controllers in the frequency domain," *WSEAS Transactions Journal of Systems and Control*, Vol. 4, No. 5, May 2009, pp. 232-242.

[15] Jaleeli, N., Vansiyck, L., Ewart, D., Fink, L., and A. G. Hoffmann, "Understanding automatic generation control," *Transactions on Power Systems*, 7(3), August 1992, pp. 1106-1111.

[16] Athay, T. M., "Generation scheduling and control," *Proceedings of the IEEE*, 75(12), December 1987, pp 1592-1605.

[17] N.L. Kothari, J. Nanda, D.P. Kothari, D. P., and D. Das, "Discrete-mode automatic generation control of a two-area reheat thermal system with new area control error," *IEEE Transaction on Power Systems*, Vol. 4, No. 9, May 1989, pp 730-736.

[18] Ramakrishna, K.S.S. and T.S. Bhatti, "Automatic generation control of single area power system with multi-source power generation," *Proc. IMechE Power and Energy*, Vol. 222, No. A, September 2007, pp. 1-11.

LIST OF REFERENCES (continued)

[19] Panda, G., Panda, S., and C. Ardil, "Automatic generation control of interconnected power system with generation rate constraints by hybrid neuro fuzzy approach," *World Academy of Science, Engineering and Technology*, Vol. 52, 2009, pp. 543-548.

[20] Eker, I., "Governors for hydro-turbine speed control in power generation: a SIMO robust design approach," *Energy Conversion and Management*, Vol. 45, 2004, pp. 2207-2221.

[21] Zavarei, M.M. and M. Jamshidi, *Time-Delay Systems: Analysis, Optimization and Applications,* Elsevier Science Publisher, Amsterdam, The Netherlands, 1987, Chapter 1, pp. 1-15.

[22] Graham, Goodwin C., Graebe, Stefen F., and Mario E. Salgado, "Control System Design," online URL: http://csd.newcastle.edu.au/chapters/Fig1_1.png Date Retrieved: March 2010

[23] U.S. Energy Information Administration, Independent Statistics and Analysis.
online URL: **http://www.eia.doe.gov/cneaf/electricity/epa/epat1p1.html**
Date Retrieved: May 2010

[24] "Basics of electrical machines," online URL:http://www.reliance.com/mtr/mtrthrmn.htm
Date Retrieved: June 2010

APPENDIXES

APPENDIX A

MATLAB M-file for designing additive weight ($W_A(s)$) to bound uncertainties for DC motor with time delay

```
% This Matlab code shows the design method used  to design the
% additive uncertainty weight which bounds the uncertainities
% present in the DC motor model

% ADDITIVE UNCERTAINTY WEIGHT DESIGN
close all;
clear all;
clc;
s=tf('s');
% Nominal Model of the DC motor
Go=(65.5)/(s*(s+34.6));
td=0.1;
set( Go, 'iodelay',td);% assigning delay
w=logspace(-2,3,100);
% Additive Uncertainity representing entire set of perturbations
figure(1)
clf
title('Additive Uncertainity')
ylabel('Magnitude (dB)')
xlabel('Frequency (rad/sec)')
set(gca,'xscale','log')
ymin=[-10 -150];
grid on
hold all
% time delays present in the DC motor
for tau=[0.05:0.01:0.15];
G=(65.5)/(s*(s+34.6));
set(G,'iodelay',tau);
H=squeeze(freqresp(G,w)-freqresp(Go,w));
plot(w,20*log10(abs(H)))
end
legend('0.05','0.06','0.07','0.08','0.09','0.10','0.11','0.12',
'0.13','0.14','0.15',3);
% Additive weight designed to bound the uncertainties
Mh=.13;
wc1=20.67;%crossover frequency
wc2=100;%pole placement frequency
Ws=tf(Mh,[1/wc1,1])*tf(1,[1/wc2,1]); %Additive Weight designed
H=squeeze(freqresp(Ws,w));
plot(w,20*log10(abs(H)),'LineWidth',2,'color','r');
hold off
```

APPENDIX B

MATLAB M-file for PID controller design to ensure robust stability in (K_p, K_i),(K_p, K_d), and (K_i, K_d)planes, respectively for the DC motor model with time delay

PID controller design function

```
function[Kp,Ki,Kd,Gc1,Gc2,Gc3,Gc11,Gc22,Gc33]=adduncpid(G,Ws,w,Kdt,Kit,Kpt,axdx,axdy,axix,axiy,axpx1,axpy2,axpx3,axpy4,axpi,axpd,axid)

% This Matlab function enables to evaluate the PID gains to obtain nominal
%stability boundary and robust stability region for the DC motor model with
time delay.
% Robust Stability region is obtained as the intersection of
% all regions inside the nominal stability boundary in the (Kp,Ki),(Kp,Kd),
% and (Ki,Kd) planes for constant values of Kp, Ki, and Kd, respectively.
% The controllers selected from the robust stability region should ensure
%that the weighted sensitivity constraint |W_A KS|_∞ <1 is satisfied.
%Authors: Manoj Gogoi, Tooran Emami, and John Watkins

%::::::EECS department Wichita State University

%%%%%%%%%%%%%%%%%%%%%%%%%%%%%%%%%%%%%%%%%%%%%%%%%%%%%%%%%%%%%%%%%%%%%%%%%%%%%%%%

% Frequency domain representation of the nominal plant model
%and the additive uncertainty weight.
s=zpk('s');
om=imag(frd(s,w));
Gp=frd(G,w);
Wp=frd(Ws,w);
Rp=real(Gp);
Ip=imag(Gp);
Gd=abs(Gp);
Wa=abs(Wp);
Gd2=Gd^2;
A=real(Wp);
B=imag(Wp);
Wa2=Wa^2;
```

APPENDIX B (continued)

```
%Nominal Stability region and Robust Stability region for
constant Kd

figure(1)
xlim(axdx);
ylim(axdy);
xlabel('K_p');
ylabel('K_i');
title(['']);
grid on;

%Nominal Stability region and Robust Stability region for
constant Ki

figure(2)
xlim(axix);
ylim(axiy);
xlabel('K_p');
ylabel('K_d');
grid on;

%Range of frequencies obtained to find a solution in (Ki,Kd)
plane

figure(3)
xlim(axpx1);
ylim(axpy2);
xlabel('w');
ylabel('K_p');
grid on;

%Nominal Stability region and Robust Stability region for
constant Kp

figure(4)
xlim(axpx3);
ylim(axpy4);
xlabel('K_i');
ylabel('K_d');
grid on;

% Obtaining the robust stability boundaries for the entire set
of uncertainties for entire frequency range.

for p=0:0.1:2*pi;
            C=(A*cos(p) - B*sin(p))*Rp;
            D=(A*sin(p) + B*cos(p))*Ip;
```

APPENDIX B (continued)

```
            Q =(Gd2+Wa2+(2*(C+D)));
            x=om*Kdt*Q ;
            P= ((-Rp-(C/Rp))/(Q));
            I= ((om*(x-(Ip+(D/Ip))))/(Q));
            figure(1)
            line('Xdata', P.responsedata(:),'Ydata',
I.responsedata(:),'color','g','LineStyle','--','linewidth',1);
            hold on;
            Kp= ((-Rp-(C/Rp))/(Q));
            Kd= ((Kit*Q)+((Ip+(D/Ip))*om))/(om^2*Q);
            figure(2)
            line('Xdata', Kp.responsedata(:),'Ydata',
Kd.responsedata(:),'color','g','LineStyle','-','linewidth',1);
            hold on;

% obtaining the range of new frequencies wi
            figure(3)
            line('Xdata', P.frequency(:),'Ydata',
P.responsedata(:),'color','g','LineStyle','--','linewidth',1);
            hold on;
            y=[mrdivide(P.responsedata(:),Kpt)-1]';
            c=abs(diff(sign(y)));
            b=size(c);
            z=ones(b);
            m=and(c,z);
            [i,j]=find(c~=0);
            k=abs(i);
            n=sum(k);
            wi=zeros(1,n);

          for i=1:n;
            wi(i)=interp1(y(j(i):j(i)+1),w(j(i):j(i)+1), 0);
            plot(wi,Kpt,'*');
          end
            Ki=-20:0.5:20;
            Kd1=Ki*0;
      for i=1:n;
            Gp1=frd(G,abs(wi(i)));
            Rp1=real(Gp1);
            Ip1=imag(Gp1);
            Wp1=frd(Ws, abs(wi(i)));
            A1=real(Wp1);
            B1=imag(Wp1);
            Gd1=abs(Gp1);
```

APPENDIX B (continued)

```
            Gd21=Gd1^2;
            Wa22=abs(Wp1);
            Wa21=Wa22^2;
            C1=(A1*cos(p) - B1*sin(p))*Rp1;
            D1=(A1*sin(p) + B1*cos(p))*Ip1;
            Q1 =(Gd21+Wa21+(2*(C1+D1)));
            Kd2=(Ki/wi(i)^2)+(Ip1 +
           (A1*sin(p)+B1*cos(p)))/(wi(i)*Q1);
         figure(4)

line('Xdata',Ki,'Ydata',Kd2.responsedata(:),'color','g');
         line('Xdata',Kd1,'Ydata',Ki,'color','g');
         hold on;
      end
 end

% Nominal Stability Boundary in (Kp ,Ki) plane

P1=-Rp;
numKp=P1;
D1=(Kdt*om*Q - Ip);
numKi=om*D1;
Kp=numKp/(Gd2);
Ki=numKi/(Gd2);
figure(1)
line('Xdata', Kp.responsedata(:),'Ydata',
Ki.responsedata(:),'color','r','linewidth',1.5);
hold on;
numKi1=0;
Kp=numKp/(Gd2);
Ki=numKi1/(Gd2);
figure(1)
line('Xdata', Kp.responsedata(:),'Ydata',
Ki.responsedata(:),'color','r','linewidth',1.5);
hold on;

%Verifying if the robust stability constraint [WaKS]<1
specifications is met

[x,y]=ginput(2)
plot(x(1,1),y(1,1),'-.b*');
plot(x(2,1),y(2,1),'-.r*');
Gc1=(x(1,1)+(y(1,1)/s)+(Kdt*s))
Gcp=frd(Gc1,w);
L=Gp*Gcp;
Se= 1/(1+L);
```

APPENDIX B (continued)

```
Sd=abs(Se);
Gcpd=abs(Gcp);
WS=Wa*Gcpd*Sd;
figure(5)
line('Xdata', WS.frequency(:),'Ydata',
WS.responsedata(:),'color','b','linewidth',1);
hold on;
figure(1)
Gc11=(x(2,1))+(y(2,1)/s)+(Kdt*s)
Gcp1=frd(Gc11,w);
L1=Gp*Gcp1;
Se1=1/(1+L1);
Sd1=abs(Se1);
Gcpd1=abs(Gcp1);
WS1=Wa*Gcpd1*Sd1;
figure(5)
line('Xdata', WS1.frequency(:),'Ydata',
WS1.responsedata(:),'color','r','linewidth',1);
hold on;
set(gca,'xscale','log');
ylim(axpi);
xlabel('frequency');
ylabel('Mag');
grid on;

%Bode Plot for nominal closed loop stability in (Kp Ki) plane

figure (8)
bode (G*Gc1);

% Nominal Stability Boundary in (Kp ,Kd) plane

P1=-Rp;
numKp=P1;
numKd=((Kit*Gd2)+(om*Ip));
Kp=numKp/(Gd2);
Kd=numKd/((om^2)*(Gd2));
figure(2)
line('Xdata', Kp.responsedata(:),'Ydata',
Kd.responsedata(:),'color','r','linewidth',1.5);
hold on;
```

APPENDIX B (continued)

```
%Verifying if the robust stability constraint [WaKS]<1
specifications is met in (Kp,Kd) plane;

[x,y]=ginput(2)
plot(x(1,1),y(1,1),'-.b*');
plot(x(2,1),y(2,1),'-.r*');
Gc2=x(1,1)+(Kit/s)+(y(1,1)*s)
Gcp=frd(Gc2,w);
Gcpd=abs(Gcp);
L=Gp*Gcp;
Se= 1/(1+L);
Sd=abs(Se);
WS=Wa*Gcpd*Sd;

%Bode Plot for (Kp Kd) plane

figure(6)
line('Xdata', WS.frequency(:),'Ydata',
WS.responsedata(:),'color','b','linewidth',1);
hold on;
figure(2)
Gc22=x(2,1)+(Kit/s)+(y(2,1)*s)
Gcp1=frd(Gc22,w);
Gcpd1=abs(Gcp1);
L1=Gp*Gcp1;
Se1=1/(1+L1);
Sd1=abs(Se1);
WS1=Wa*Gcpd1*Sd1;
figure(6)
line('Xdata', WS1.frequency(:),'Ydata',
WS1.responsedata(:),'color','r','linewidth',1);
hold on;
set(gca,'xscale','log');
ylim(axpd);
xlabel('frequency');
ylabel('Mag');
title('[WpS]<1 in PDplane');
grid on;
figure (9)
bode (G*Gc2);

%Nominal Stability Boundary in (Ki ,Kd) plane

P1=-Rp;
numKp=P1;
Kp=numKp/Gd2;
```

APPENDIX B (continued)

```
figure(3)
line('Xdata', Kp.frequency(:),'Ydata',
Kp.responsedata(:),'color','r','linewidth',1.5);
        y=[mrdivide(Kp.responsedata(:),Kpt)-1]';
        c=abs(diff(sign(y)));
            b=size(c);
            z=ones(b);
            m=and(c,z);
            [i,j]=find(c~=0);
            k=abs(i);
            n=sum(k);
            wi=zeros(1,n);

for i=1:n;
    wi(i)=interp1(y(j(i):j(i)+1),w(j(i):j(i)+1), 0);
    plot(wi,Kpt,'*');

end
        Ki=-20:0.1:20;
        Kd1=Ki*0;
    for i=1:n;
        Gp1=frd(G,abs(wi(i)));
        Rp1=real(Gp1);
        Ip1=imag(Gp1);
        Gd1=abs(Gp1);
        Gd21=Gd1^2;
        Kd2=Ki/wi(i)^2+Ip1/(wi(i)*Gd21);
        figure(4)
        line('Xdata',Kd1,'Ydata',Ki,'color','r');

line('Xdata',Ki,'Ydata',Kd2.responsedata(:),'color','r');
    end

%Verifying if the robust stability constraint [WaKS]<1
%specifications is met in (Ki,Kd) plane;
[x,y]=ginput(2)
plot(x(1,1),y(1,1),'-.b*');
plot(x(2,1),y(2,1),'-.r*');
Gc3=Kpt+(x(1,1)/s)+(y(1,1)*s)
Gcp=frd(Gc3,w);
Gcpd=abs(Gcp);
L=Gp*Gcp;
Se= 1/(1+L);
Sd=abs(Se);
```

APPENDIX B (continued)

```
WS=Wa*Gcpd*Sd;
figure(7)
line('Xdata', WS.frequency(:),'Ydata',
WS.responsedata(:),'color','b','linewidth',1);
hold on;
figure(4)
Gc33=Kpt+(x(2,1)/s)+(y(2,1)*s)
Gcp1=frd(Gc33,w);
Gcpd1=abs(Gcp1);
L1=Gp*Gcp1;
Se1=1/(1+L1);
Sd1=abs(Se1);
WS1=Wa*Gcpd1*Sd1;

%Bode Plot for (Ki Kd) plane
figure(7)
line('Xdata', WS1.frequency(:),'Ydata',
WS1.responsedata(:),'color','r','linewidth',1);
hold on;
set(gca,'xscale','log');
 ylim(axid);
 xlabel('frequency');
 ylabel('Mag');
 title('MAGNITUDE OF [WpS] in ID plane');
 grid on;
figure (10)
bode (G*Gc3);
```

APPENDIX C

MATLAB M-file for PID compensator design for DC motor with time delay (script file)

```
% In this section the script file required to call the function
% is being illustrated.

close all;
clear all;
clc;
s=tf('s');
% Nominal plant transfer function
G=(65.5)/(s*(s+34.6));
td=0.1;
set( G, 'iodelay',td);% assigning delay
w=0.01:0.05:30;
Ws=(0.13)/(0.0004838*s^2 + 0.05838*s + 1); % Additive weight
Kdt=0.2;
Kit=1;
Kpt=0.5;
% Define PI plane  axes range
axdx=[-1 10];
axdy=[0 40];
%Define PD plane axes range
axix=[-1 10];
axiy=[-0.6 0.7];
%Define Kp versus frequency  axes range
axpx1=[0 25];
axpy2=[0 9];
%Define ID plane axes range
axpx3=[-1 8];
axpy4=[-0.8 0.8];
% Y-axis for [WaKS<1] analysis
axpi=[0 1.3];
axpd=[0 1.3];
axid=[0 1.3];

%Function Call
[Kp,Ki,Kd,Gc1,Gc2,Gc3,Gc11,Gc22,Gc33]=adduncpid(G,Ws,w,Kdt,Kit,K
pt,axdx,axdy,axix,axiy,axpx1,axpy2,axpx3,axpy4,axpi,axpd,axid);
```

APPENDIX D

MATLAB M-file for PI controller design to ensure robust stability in (K_p, K_i) plane for the single area non-reheat steam generator unit

```
function[Kp,Ki,Gc1,Gc11]=addunclfc(G,Ws,w,Kdt,axd1,axd2,axpi)
% In this MATLAB code we design the entire range of PI
%controller gains which will ensure that the design goal of
%obtaining a robust stable closed loop system
%The presence of parametric uncertainties in the plant model is
%assumed.
%Simulation results show the ability to obtain PI controllers
which will satisfy the robust stability constraint |W_A KS|_∞ <1.

function[Kp,Ki,Gc1,Gc11]=addunclfcnew(G,Ws,w,Kdt,axd1,axd2,axpi)

s=zpk('s');
om=imag(frd(s,w));
Gp=frd(G,w);
Wp=frd(Ws,w);
Rp=real(Gp);
Ip=imag(Gp);
Gd=abs(Gp);
Gd2=Gd^2;
A=real(Wp);
B=imag(Wp);
Wap=abs(Wp);
Wa2=Wap^2;

figure(2)
xlim(axd1);
ylim(axd2);
xlabel('K_p');
ylabel('K_i');
title('PI Controller region for Robust stability and Nominal
stability  for perturbed plant');
grid on;

figure(6)
title(' Fig(6)-----Closed loop stabilty  for Kp= and Ki= ');
figure(7)
title(' Fig(7)-----Closed loop stabilty  for Kp= and Ki= ');
figure(5)
title(' Fig(5)-----[WaKS]<1 specifications in PI plane ');
```

APPENDIX D (continued)

```
%PI plane stability region

 for p=0:0.1:2*pi;
            C=(A*cos(p) - B*sin(p))*Rp;
            D=(A*sin(p) + B*cos(p))*Ip;
            Q =(Gd2+Wa2+(2*(C+D)));
            x=om*Kdt*Q ;
            P= ((-Rp-(C/Rp))/(Q));
            I= ((om*(x-(Ip+(D/Ip))))/(Q));
            figure(2)
            line('Xdata', P.responsedata(:),'Ydata',
I.responsedata(:),'color','g','LineStyle','-','linewidth',1);
            hold on;
 end
P1=-Rp;
numKp=P1;
D1=Kdt*om*(Gd2)-Ip;
numKi=om*D1;
Kp=numKp/Gd2;
Ki=numKi/Gd2;
figure(2)
line('Xdata', Kp.responsedata(:),'Ydata',
Ki.responsedata(:),'color','r','linewidth',1.5);
hold on;
D2=0*om*(Gd2)-Ip;
Kp1= D2;
Ki1=numKi/Gd2;
figure(2)
line('Xdata', Kp1.responsedata(:),'Ydata',
Ki1.responsedata(:),'color','r','linewidth',1);

%Check if we meet our [WaKS]<1 specifications in PI plane
[x,y]=ginput(1)
plot(x(1,1),y(1,1),'-.b*');
Gc1=(x(1,1)+(y(1,1)/s)+(Kdt*s))
Lo=G*Gc1;
figure(3)
bode(Lo);
grid on;
Gcp=frd(Gc1,w);
L=Gp*Gcp;
Se= 1/(1+L);
Sd=abs(Se);
Gcpd=abs(Gcp);
```

APPENDIX D (continued)

```
WS=Wap*Gcpd*Sd;
figure(5)
line('Xdata', WS.frequency(:),'Ydata',
WS.responsedata(:),'color','b','LineStyle','-','linewidth',1);
hold on;
set(gca,'xscale','log');
ylim(axpi);
xlabel('frequency');
ylabel('Mag');
grid on;
```

APPENDIX E

MATLAB M-file for designing additive weight ($W_A(s)$) and the script file for the single area non-reheat steam generator unit.

```
% This MATLAB code is used to design additive uncertainty weight
% for 20% parameter uncertainties present and which enables us
%to evaluate the PI stability boundary and robust stability
%region for a single area non-reheat steam generator unit.
%(20% PARAMETRIC UNCERTAINTY)
%Authors: Manoj Gogoi, Tooran Emami, and John Watkins
%EECS department Wichita State University


close all;
clear all;
clc;
s=tf('s');
D1=0.015;%Load damping constant
R1=3.00;%Speed Droop characteristics
Tch=0.5;%Turbine time constant
M=0.1667;%Inertia constant
Tg=0.08;%Governor time constant
G1=1/(1+s*Tg);%Governor transfer function
G2=1/(1+s*Tch);%Turbine transfer function
G3=1/(M*s+D1);%Generator transfer function
Tpi=(2*pi)/s;%Integrator added
T12=0.20;%per unit power interchange between area1 and area 2
T13=0.25;%per unit power interchange between area1 and area 3
W1o=0.01;%nominal load change
T1=(T12)+(T13);% Total power interchange
B1= (1/R1)+D1;%Frequency Bias factor
Go=feedback((1/R1),(G3*G2*G1),-1);% feedback loop including 1/R1
Go1=feedback( 1,(Tpi*T1*G3),-1);% feedback loop including Tpi
and T1

% Nominal plant model
G = ((Tpi*T1)+ B1)*G3*G2*G1*(Go1+Go);
w=0.01:0.01:20;% Frequency range
figure(1)
clf
ylabel('Magnitude (dB)')
xlabel('Frequency (rad/sec)')
set(gca,'xscale','log')
grid on
hold all
Tmh=[];
```

APPENDIX E (continued)

```
% Representing 20% uncertainty in the governor time, rotating
mass-load model
for Tg=[0.064:0.01:0.096];% uncertainty  in the governor time
     for     M=[0.133:0.001:0.199];% uncertainty  in the inertia
         for  D=[0.012:0.01:0.018];% uncertainty  in speed droop
              G1=1/(1+s*Tg);
              G3=1/(M*s+D);
              %perturbed plant model
              Gp=((Tpi*T1)+ B1)*G3*G2*G1*(Go1+Go);
              H=squeeze(freqresp(Gp,w)-freqresp(G,w));
              plot(w,20*log10(abs(H)));
              Tmh=[M D];
         end
     end
end

%Obtaining additive weight Transfer function
G11=1/(1+s*(0.064));
G31=1/((0.133)*s+(0.012));
Ws=((((Tpi*T1)+ B1)*G31*G2*G11*(Go1+Go))-Gp);
H=squeeze((freqresp(Ws,w)));
plot(w,20*log10(abs(H)),'LineWidth',2,'color','k');
hold off
Kdt=0;
axd1=[0 0.07];
axd2=[0 0.25];
axpi=[0 1.3];


%Function Call ( Script file )
[Kp,Ki,Gc1]=addunclfcnew(G,Ws,w,Kdt,axd1,axd2,axpi);
```